Fall 2018

Practical dwell times for switched system stability with smart grid application

William Roy St. Pierre

Department:

PRACTICAL DWELL TIMES FOR SWITCHED SYSTEM STABILITY WITH SMART GRID APPLICATION

by

WILLIAM ROY ST. PIERRE

A THESIS

Presented to the Graduate Faculty of the

MISSOURI UNIVERSITY OF SCIENCE AND TECHNOLOGY

In Partial Fulfillment of the Requirements for the Degree

MASTER OF SCIENCE

in

ELECTRICAL ENGINEERING

2018

Approved by

Jonathan Kimball, Advisor
Levent Acar
Mehdi Ferdowsi

PUBLICATION THESIS OPTION

This thesis consists of the following two articles which have been submitted for publication, or will be submitted for publication as follows:

Paper I: Pages 8-26 have been accepted by the 2018 American Control Conference.

Paper II: Pages 27-52 are intended for submission to IEEE Transactions on Control Systems Technology.

ABSTRACT

Switched systems are encountered throughout many engineering disciplines, but confirming their stability is a challenging task. Even if each subsystem is asymptotically stable, certain switching sequences may exist that drive the overall system states into unacceptable regions. This thesis contains a process that grants stability under switching to switched systems with multiple operating points. The method linearizes a switched system about its distinct operating points, and employs multiple Lyapunov functions to produce modal dwell times that yield stability. This approach prioritizes practicality and is designed to be useful for large systems with many states and subsystems due to its ease of algorithmic implementation. Power applications are particularly targeted, and several examples are provided in the included papers that apply the technique to boost converters, electric machines, and smart grid architectures.

ACKNOWLEDGMENTS

I am immensely grateful to my advisor, Dr. Kimball, for his persistent support of this work, and for all the time he invested in processing new ideas and developments with me. His insight guided the entire process and restored my resolve when numerous obstacles emerged. I also extend gratitude to my committee members, Dr. Acar and Dr. Ferdowsi, for always being available to consult on control theory and power systems.

I am very thankful for the friendship and solidarity I received from all fellow students in Dr. Kimball's lab. I especially thank Bokang Zhou for his many contributions to the ideas in this thesis.

Finally, I thank my wife and my family for their patience and support as I pondered switched system theory and shared my excitement with them. Their willingness to participate in my musings affirmed me and inspired perseverance.

TABLE OF CONTENTS

Page

PUBLICATION THESIS OPTION iii

ABSTRACT iv

ACKNOWLEDGMENTS v

LIST OF ILLUSTRATIONS ix

LIST OF TABLES x

SECTION

1. INTRODUCTION 1

2. LITERATURE REVIEW 3

2.1. DWELL TIME TECHNIQUES 3

2.2. MULTIPLE LYAPUNOV FUNCTIONS 4

2.3. MULTIPLE EQUILIBRIA 5

2.3.1. Lyapunov Analysis 5

2.3.2. Modal Dwell Times from Set Theory 6

2.3.3. Practical Stability for Power Systems 6

PAPER

I. MINIMUM DWELL TIMES FOR THE STABILITY OF SWITCHED SYSTEMS WITH MULTIPLE STABLE OPERATING POINTS 8

ABSTRACT 8

1. INTRODUCTION 9

2. BACKGROUND ON LYAPUNOV STABILITY 10
3. LYAPUNOV LEVEL SETS FOR STABILITY ANALYSIS 12
3.1. LEVEL SETS AND MOTIVATION 12
3.2. DEFINING LEVEL SETS 13
3.3. DETERMINING DWELL TIMES 14
3.4. CHOOSING α AND γ TERMS 15
3.5. ILL-CONDITIONED SYSTEMS 17
4. EXAMPLES 20
4.1. BOOST CONVERTER 20
4.2. INDUCTION MACHINE 21
ACKNOWLEDGEMENTS 24
REFERENCES 25

II. PRACTICAL DWELL TIMES FOR SWITCHED SYSTEMS WITH MULTIPLE OPERATING POINTS FOR MICROGRID STABILITY 27
ABSTRACT 27
1. INTRODUCTION 27
2. BACKGROUND AND MOTIVATION 30
2.1. PRELIMINARIES 30
2.2. MOTIVATING ANALYSIS OF UNSTABLE SWITCHING 31
3. MAIN RESULT 32
4. PRACTICAL APPLICATION 34
4.1. SELECTING BALL SIZES 34
4.2. CALCULATION OF DWELL TIMES 36
4.3. ILL-CONDITIONED SYSTEMS 38
4.4. DISSCUSSION AND COMPARISON 39
5. DWELL TIMES FROM SETTLING TIMES 42

6. SIMULATIONS 43
6.1. BOOST CONVERTER 43
6.2. MICROGRID 46
6.3. POWER GRID 47
7. CONCLUSION 50
ACKNOWLEDGEMENTS 50
REFERENCES 51

SECTION

3. SUMMARY AND CONCLUSIONS 53

APPENDIX 56

REFERENCES 79

VITA 81

LIST OF ILLUSTRATIONS

Figure Page

PAPER I

1. An illustration of a mode with associated objects..... 12
2. Depiction of two mode system with possible balls 13
3. Ellipsoid with axis lengths 15
4. Algorithm flowchart..... 17
5. An ill-conditioned mode 17
6. Ill-conditioned system with possible state locations and the T ellipsoid shown... 18
7. Diagram of boost converter 20
8. Stable operating points and balls for the boost converter system 21

PAPER II

1. Depiction of a mode with associated objects 33
2. Example collection of four modes with balls 35
3. Illustration of procedure 37
4. An ill-conditioned mode 38
5. Boost converter circuit 43
6. Switched boost converter under minimum dwell times 44
7. Unstable behavior without minimum dwell times 45
8. Microgrid under minimum dwell times 48
9. Seven node power grid 48

SECTION

3.1. Boost converter switching with unknown modes 54

LIST OF TABLES

Table Page

PAPER I

1. Induction motor model symbols and values 23

SECTION

1. INTRODUCTION

A switched system is a system with dynamics drawn from one of many potential subsystems and a switching signal that discretely switches between these continuous subsystems in selecting the active dynamics at every time instant. This switching nature complicates the question of stability because even if all subsystems are exponentially stable, the overall system states can often be driven arbitrarily distant from equilibria by certain switching signals. To ensure stability, one must either demonstrate system stability for a particular switching sequence or identify a set of switching sequences under which the system is stable.

This theoretical problem is relevant in many applied fields, especially in power systems. The advent and ongoing development of the Smart Grid has been distinguished by an increase in distributed energy resources and the synthesis of microgrids into the overall grid. A defining characteristic of microgrid systems is their ability to operate in either islanded or grid-connected configurations, with a switching action present in the transition between these modes.

Also integral to the Smart Grid is its enhanced cyber component, which qualifies the Smart Grid as a cyber-physical system. While the cyber component enables greater monitoring and control of power production, it also opens up the grid to new security threats. In one possible cyber-enabled physical attack, an attacker could gain online control of a microgrid islanding command, and use it to physically switch the system into instability, potentially causing power failure. By modelling and evaluating the grid as a switched

system, stability standards can be produced, and switching actions can be monitored to ensure compliance. In this way, malicious switching attacks or inadvertent uncontrolled switching can be identified and avoided to maintain stability.

With such motivation, this thesis develops a practical method for switched system analysis, which results in restrictions on the elapsed time between switching events. Observing these switching rules will guarantee sustained stability. The approach is designed to be easily implementable and attractive to the working power systems engineer. To emphasize the underlying inspiration, many examples are drawn from power applications and processed via the created algorithm.

2. LITERATURE REVIEW

The stability of switched systems has been studied extensively. Two broad problems have received the most attention: stability and stabilizability. Solutions to the stability problem seek to uncover switching signals that achieve system stability, while stabilizability results reveal which switched systems are possible to stabilize with some switching signal. This thesis is concerned with the stability problem. Several general techniques exist for solving this problem, but the two most prominent among these are those using dwell times and those using Lyapunov function values.

2.1. DWELL TIME TECHNIQUES

In the first approach, restrictions are placed on the elapsed time between switching events, known as the dwell time. If a switching signal satisfies these conditions, it is shown that the system will remain stable. Several variations on this theme exist, such as the notions of minimum dwell time, average dwell time, and modal dwell times.

Minimum dwell time methods require that each dwell time be greater than a minimum threshold over the entire switching sequence. For example, (1) presents a minimum dwell time formulation that will guarantee system stability as long as the proper dwell time is observed. However, this technique was created for systems in which all subsystems share an operating point and is not immediately extendable to the multiple equilibria case.

In a more relaxed style, average dwell time laws require that the dwell times maintain a sufficiently large average. These were first introduced in (2), and several methods of calculating average dwell times exist, such as in (3). Recently, (4) generalized results for slowly time-varying systems to attain average dwell times for switched linear systems. Once again, these works do not confront the issue of switched systems with multiple operating points.

Finally, modal dwell times assign a unique minimum dwell time to each system mode so that the required switching time elapsed depends on the current mode of the system. One procedure developed in (5; 6) merges the concepts of modal and average dwell times and shows that linear switched system stability can be achieved if the total number of switches to a particular mode is limited on the average of its total active time in the system history.

2.2. MULTIPLE LYAPUNOV FUNCTIONS

Strategies that monitor Lyapunov function values typically seek either one Lyapunov function that applies to all system modes (which is only obtainable if all modes share an operating point) or a distinct Lyapunov function for each subsystem. These tactics usually consider the values of the Lyapunov functions at each switching moment and then draw conclusions on the pattern. For example, (7) extends traditional Lyapunov theory to switched systems with multiple Lyapunov functions. The authors show that if all Lyapunov functions are nonincreasing over all time instants that their respective modes are activated, then the system is stable in the sense of Lyapunov.

Although this is suited only to switched systems with a single operating point, (7) briefly remarks that it could be extended to multiple operating points when certain conditions are met. Interestingly, existing techniques for such systems (including those in this thesis) usually work because they indirectly verify this principle. In fact, traditional dwell time approaches often limit switching signals to those that produce Lyapunov behavior satisfying conditions like those in (7), so multiple Lyapunov functions are almost always relevant.

Other analyses using multiple Lyapunov functions exist as well, but they are once again typically limited to switched systems with a single operating point. The nonincreasing Lyapunov values condition is relaxed in (8), and multiple Lyapunov functions are used to prove an upper bound on the minimum dwell time. In (9), multiple Lyapunov functions are used to expand the set of known stabilizing switching signals beyond those revealed by minimum or average dwell times. Similarly, (10) develops Lyapunov methods for

identifying sets of switching signals that grant uniform stability. More Lyapunov solutions are described in (11), and many more methods for switched systems with a single operating point are surveyed in (12; 13).

2.3. MULTIPLE EQUILIBRIA

Most real-world switched systems are nonlinear, and their subsystems rarely share an equilibrium. Stability techniques are made more practical when adapted to this case. Several works have attempted this, and they essentially attain the *practical stability* introduced in (14; 15). A system is practically stable under a given switching signal if initial states in a predefined set result in a trajectory that remains in a closed superset for all time. When the switching signal is controlled, (14) formulates two switching sequences that can be used for practical stability.

In many cases, including the Smart Grid, switching is uncontrolled or subject to uncontrolled phenomena. Switching signals cannot be designed here, but they can be watched for behavior that disregards imposed restrictions. Several papers pursue this, and each has some overlap with the ideas in this thesis.

2.3.1. Lyapunov Analysis. First, (16) demonstrates practical stability using multiple Lyapunov functions for each mode. From these, several sets are constructed that ultimately render a minimum dwell time. The sets are similar to those in this thesis, but some differences exist in the derivations which pose practical challenges. First, for N subsystems, (16) requires solving N^2 many constrained optimization problems. This is computationally expensive for systems with large numbers of modes, like the Smart Grid. This thesis requires only one constrained optimization for any number of modes. Also, the dwell time in (16) can be rather conservative, which is detailed in Paper II. Being a minimum dwell time makes it even more conservative, but the introduction of modal dwell times can allay this.

2.3.2. Modal Dwell Times from Set Theory. In another procedure, (17) introduces maximally invariant sets as the largest sets of possible initial state values for which states remain in a predefined superset $\mathcal{X}$. The process suggests computing a maximally invariant set for each system mode and using modal dwell times that guarantee all switching actions occur within the intersection of the invariant sets. In this way, states are restricted to $\mathcal{X}$ for all time, which is a practical stability.

Maximally invariant sets can be difficult to compute, so the authors set forth methods for specific cases. For affine systems with different equilibria, the authors show how to compute maximally invariant sets that are polytopes as long as $\mathcal{X}$ is a polytope. While this can produce non-conservative dwell times, the polytopes become very complex and difficult to analyze in high dimensions. As an alternative, (17) recommends using Lyapunov level sets as suboptimal invariant sets. The recommendation is to select two level sets for each mode: a larger one that is a subset of $\mathcal{X}$ and another that is contained in the intersection of the larger Lyapunov sets over all modes. Using bounds on the Lyapunov derivatives, modal dwell times can be computed that restrict the state to the union of larger Lyapunov sets.

The challenge in this strategy is selecting the Lyapunov sets so that they satisfy their subset requirements. This is not a trivial problem when working with numerous ellipsoidal level sets in high dimensions. The approach developed in this thesis relies on a similar intuition as (17), but proposes a more natural and easily implementable way to select Lyapunov level sets.

2.3.3. Practical Stability for Power Systems. Finally, a practically-focused process for accomplishing practical stability is presented in (18). The author's applications are similar to those in this thesis, as shown by the grid example in (19). The method drafts a minimum dwell time that achieves desired behavior in the multiple Lyapunov functions, and proves practical stability. The technique is for finite, predetermined time frames, and does not easily extend to the infinite horizon case. This is a practical obstacle because many systems require perpetual monitoring.

The ideal practical method for switched system stability is computationally efficient, robust in implementation, and perpetual in operation. The following publications develop a method that targets these qualities.

PAPER

I. MINIMUM DWELL TIMES FOR THE STABILITY OF SWITCHED SYSTEMS WITH MULTIPLE STABLE OPERATING POINTS

W. R. St. Pierre and J. W. Kimball

% Department of Electrical Engineering

Missouri University of Science and Technology

Rolla, Missouri 65409–0050

Tel: 573–341–6622, Fax: 573–341–4115

Email: wrsthf@mst.edu

ABSTRACT

This work outlines a practical process, based on dwell times, for ensuring the stability of non-linear switched systems with a different stable equilibrium for each mode. Relevant Lyapunov theorems are discussed, followed by a derivation of an algorithm that determines dwell times for each system mode for guaranteeing stability. An analysis of algorithm parameters and potentially troublesome systems is then included. Finally, two examples are drawn from power electronics and electric machinery and processed by the proposed method. Application of this approach will both grant confidence in switched system stability and warn of possible unstable system behavior when appropriate.

Keywords: convection

1. INTRODUCTION

The ubiquity of switched systems has inspired a considerable volume of research into their stability. Much of this work explores switched systems whose discrete modes all produce the same stable operating point. However, many switched systems contain a different stable operating point for each discrete mode, and these warrant their own methods of stability assurance. Lyapunov stability techniques can ensure that each of a system's individual operating points are stable, but a particular sequence of switching could still drive the states into an unstable region. This paper presents a method for detecting potentially unstable behavior due to switching in non-linear switched systems with multiple stable equilibria.

For systems in which all modes share a common equilibrium point, switching stability has been explored extensively. Much of the literature on this subject involves the concept of dwell time, which is the amount of time that passes between consecutive switching events. If all subsystems are individually stable, then there exists a minimum dwell time that guarantees stability under switching if observed between all consecutive switching events. Several Lyapunov based methods of calculating this dwell time are available (1; 20). Also, stability can be achieved when the time between consecutive switches is limited on the average, which is known as the average dwell time (2; 3). In yet another approach, multiple Lyapunov functions are used to ascertain system stability (7). More stability results of this kind are surveyed in (12).

Unfortunately, these methods do not apply to systems with multiple equilibria, for which stability results are more rare. On this topic, (16) outlines a way to obtain a minimum dwell time which, if enforced after every switching action, guarantees that the states will converge to a superset of the stable equilibria. However, this process is difficult to implement algorithmically for a general system as it relies on analytical processing of multiple Lyapunov functions.

Alternatively, a set-theoretic method of determining modal dwell times (dwell times that depend on the currently active subsystem) for nonlinear switched systems is developed in (17). This strategy is created for the case in which a region of admissible trajectories is known, and it is necessary to restrict states to this region. However, the sets involved in the process can be very difficult to compute, especially for high order systems. As a practical concession, (17) recommends the use of suboptimal Lyapunov level sets to achieve the result, but an implementable algorithm for selecting these sets is not detailed, and confirming that they lie within the region of admissible states can be difficult.

This paper presents a practical process that produces dwell times from multiple Lyapunov functions, and ensures stability for switched systems with multiple equilibria. It is designed for easy implementation. The dwell times discussed in this paper are modal, as found in (17), so the required dwell time in a particular switching interval is determined by the active mode in that interval. The type of stability is also in the spirit of (16), (17): observing the determined dwell times will restrict the state trajectory to a finite region about the operating points.

2. BACKGROUND ON LYAPUNOV STABILITY

An equilibrium point of a time invariant system is asymptotically stable if there exists a continuously differentiable, positive-definite, scalar function $V(\mathbf{x})$ such that $\dot{V}(\mathbf{x}) < 0$. This function $V(\mathbf{x})$ is known as a Lyapunov function. The Lyapunov Equation for a linear system $\dot{\mathbf{x}} = \mathbf{A}\mathbf{x}$ is:

$$\mathbf{A}^{\mathbf{T}}\mathbf{P} + \mathbf{P}\mathbf{A} = -\mathbf{Q} \tag{1}$$

Here, $\mathbf{Q}$ is any positive definite matrix. If there exists a positive-definite and symmetric matrix $\mathbf{P}$ that satisfies the Lyapunov equation, then the system $\dot{\mathbf{x}} = \mathbf{A}\mathbf{x}$ is asymptotically stable at the origin, and $V(\mathbf{x}) = \mathbf{x}^{\mathbf{T}}\mathbf{P}\mathbf{x}$ is a valid Lyapunov function for the linear system.

For a non-linear system, Lyapunov functions of a linearization of the system can show local stability of the original system. Let $\mathbf{x} = \mathbf{f}(\mathbf{x}, \mathbf{u})$ be a non-linear system. Suppose the system is in mode 1 with constant input $\mathbf{U_1}$ that produces equilibrium $\mathbf{X_1}$. Then $\tilde{\mathbf{x_1}} = \mathbf{A_1}\tilde{\mathbf{x_1}}$ is a linearization of the system, where $\mathbf{A_1}$ is the Jacobian of the system evaluated at $\mathbf{X_1}$ and $\mathbf{U_1}$ and $\tilde{\mathbf{x_1}} = \mathbf{x} - \mathbf{X_1}$ exists to shift to a coordinate system where $\mathbf{X_1}$ is at the origin. If a Lyapunov function $V(\mathbf{x}) = \tilde{\mathbf{x}}^\mathbf{T}\mathbf{P}\tilde{\mathbf{x}}$ is found from the Lyapunov equation for this linearized system, then the non-linear system is locally stable about $\mathbf{X_1}$.

The most conservative decay rates to each system equilibrium may be found from the upper bound on $\dot{V}(\mathbf{x})$:

$$\dot{V}(\mathbf{x}) \leq -\frac{\lambda_{min}(\mathbf{Q})}{\lambda_{max}(\mathbf{P})}V(\mathbf{x}) \tag{2}$$

where $\lambda_{max}(\mathbf{P})$ is the greatest eigenvalue of the matrix $\mathbf{P}$ and $\lambda_{min}(\mathbf{Q})$ is the smallest eigenvalue of $\mathbf{Q}$, as shown in (21). Setting these two terms strictly equal to each other and solving the resulting differential equation gives

$$V(\mathbf{x}) = V_0 \exp\left(-\frac{\lambda_{min}(\mathbf{Q})}{\lambda_{max}(\mathbf{P})}t\right) \tag{3}$$

where V_0 is some initial level set value of $V(\mathbf{x})$. This shows that a worst-case scenario time constant for mode n is

$$\lambda_n = \frac{\lambda_{max}(\mathbf{P_n})}{\lambda_{min}(\mathbf{Q_n})} \tag{4}$$

which is the slowest possible rate at which the system states could decay from the level set $V(\mathbf{x}) = V_0$.

3. LYAPUNOV LEVEL SETS FOR STABILITY ANALYSIS

3.1. LEVEL SETS AND MOTIVATION

This section introduces the proposed method for stability analysis. Suppose that each mode $n \in \{1, 2, ..., N\}$ of a non-linear switched system is asymptotically stable. For each subsystem n, a linearization may be obtained and a Lyapunov function $V_n(\mathbf{x})$ may be found from the Lyapunov equation, with $\mathbf{Q}$ as the appropriately dimensioned identity matrix. As long as the states are sufficiently close to $\mathbf{X_n}$, they will converge no slower than the exponential rate λ_n set by the Lyapunov function. However, if the states are not sufficiently close, they may never converge to $\mathbf{X_n}$ because the linearization may be inaccurate.

A level set of $V_n(\mathbf{x})$ is defined as $\{x : V_n(\mathbf{x}) = C\}$ for a constant C, which is the size of the level set. These level sets are ellipsoids centered on their respective operating points and, for each system mode, two different level sets of the corresponding Lyapunov function will be chosen in a manner soon to be introduced. Call the larger of the two H and the smaller h. Let the ball inscribed in H be called B with radius R, and let the ball circumscribed about h be called b with radius r. This is done to simplify future operations.

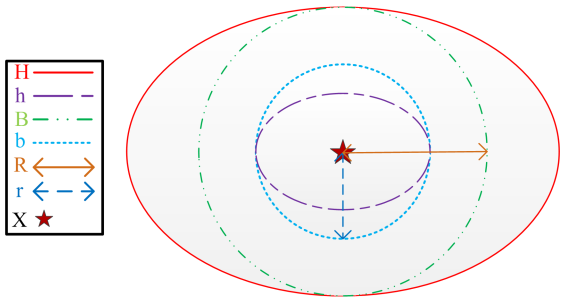

Figure 1. An illustration of a mode with associated objects.

The condition is also imposed that $\cup_{n=1}^{N} b_n \subseteq \cap_{n=1}^{N} B_n$. With this structure in mind, suppose that the system states initially rest at equilibrium $\mathbf{X_1}$ corresponding to mode 1 before the system is switched to $\mathbf{X_2}$. Since b_1 is within B_2 which is within H_2, the states will decay to b_2 after an amount of time given by the time constant for mode 2, because

they will decay to h_2 by the Lyapunov local asymptotic stability, and $h_2 \subseteq b_2$. If, after this time, the system is switched to $\mathbf{X_3}$, the same reasoning again ensures that the states will successfully decay to be within b_3 in a known length of time.

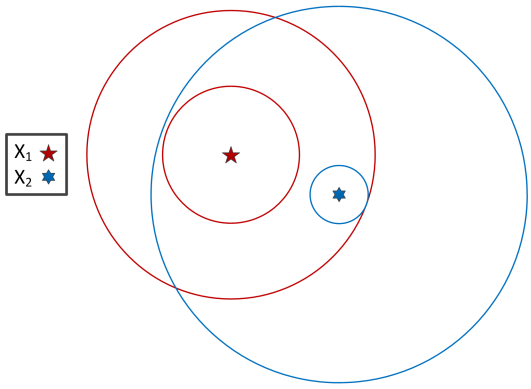

Figure 2. Depiction of two mode system with possible balls

With this established, and since the time constants for each mode are known, the system will remain in $\cup_{i=1}^{N} H_i$ as long as the appropriate amount of time passes between each switching action. This dwell time is denoted τ_n for mode n. Whenever the system switches to mode n, at least τ_n should pass before another switching action occurs. Switching behavior that consistently does not wait for the dwell times to pass might indicate a threat to system stability.

3.2. DEFINING LEVEL SETS

Before calculating these dwell times, the procedure for selecting Lyapunov level sets for each mode must be discussed. There are two criteria that influence this process. First, as mentioned, the linear approximations used are not globally valid, which means H_n needs to be "sufficiently close" to $\mathbf{X_n}$ for this approach to work. Second, the necessary dwell time between switching actions should be as small as possible. The dwell time for a mode depends on its time constant and the size of H_n relative to h_n. As H_n and h_n approach the same size, the time required for states to decay between them is decreased. Thus, both the

size of H_n and the size ratio of H_n to h_n should be reduced, which corresponds to reducing R_n and $\frac{R_n}{r_n}$. This must be done while satisfying the original constraint $\cup_{n=1}^{N} b_n \subseteq \cap_{n=1}^{N} B_n$. This is a multi-objective constrained optimization problem, which in general has no absolute solution. However, defining a function whose minimization accomplishes all objectives to varying degrees yields a Pareto optimal solution (22).

Consider the following function.

$$F = \sum_{i=1}^{N} (\alpha_i)(\frac{R_i}{r_i}) + \gamma_i R_i \tag{5}$$

The α and γ terms above are the assigned weights of each objective. Minimizing this function is known as scalarization, which results in a Pareto optimal solution. Adjusting the α and γ weights adjusts the Pareto optimum. Thus, the weights are typically chosen according to the relative importance of minimizing each term (22). This will be discussed shortly.

3.3. DETERMINING DWELL TIMES

Computing the dwell times for each mode first requires finding the magnitudes of H_i and h_i for all $i \in \{1, 2, ..., N\}$ using R_i and r_i. For a positive-definite symmetric matrix $\mathbf{P}$ in $V(\mathbf{x}) = \mathbf{x^T P x}$, there exists a coordinate rotation $\mathbf{y} = \mathbf{W x}$ such that $V(\mathbf{y}) = \mathbf{y^T E y}$, where $\mathbf{E}$ is the diagonal matrix of eigenvalues of $\mathbf{P}$. Then for level set $V(\mathbf{y}) = C$, the largest and smallest semi-principal axis lengths of the corresponding ellipsoid are, respectively,

$$Z = \sqrt{\frac{C}{\lambda_{min}(\mathbf{P})}};\ z = \sqrt{\frac{C}{\lambda_{max}(\mathbf{P})}}. \tag{6}$$

For mode n, because B_n is inscribed in H_n and b_n is circumscribed about h_n, $R_n = z$ for H_n and $r_n = Z$ for h_n. If C_n is the magnitude of H_n and c_n is that of h_n, then

$$C_n = R_n^2 \lambda_{max}(\mathbf{P_n});\ c_n = r_n^2 \lambda_{min}(\mathbf{P_n}) \tag{7}$$

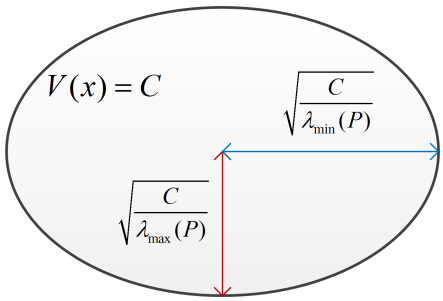

Figure 3. Ellipsoid with axis lengths

In the present case, B_n is inscribed in the larger level set chosen for mode n, and b_n is circumscribed about the smaller one. Therefore the maximum possible time to decay from B_n to b_n is the time to decay from H_n to h_n given λ_n. Combining (3) and (7), the maximum time τ_n is

$$\tau_n = -\lambda_n \ln\left(\frac{r_n^2 \lambda_{min}(\mathbf{P_n})}{R_n^2 \lambda_{max}(\mathbf{P_n})}\right) \tag{8}$$

In this way, the dwell times for each mode can be found and considered for practicality.

3.4. CHOOSING α AND γ TERMS

In order to select level sets and calculate dwell times, the α and γ terms in (5) must be chosen. In general there is no known way to predict how the weights in a scalarization problem will affect the Pareto optimum, and the relative "importance" of minimizing each term may not scale evenly to the weights. In this case there are only two types of terms to be minimized (Of the R_n and $\frac{R_n}{r_n}$ forms), so α_n will scale well to the relative importance of $\frac{R_n}{r_n}$ compared to similar terms, and γ_n will do likewise for terms of the R_n form.

For mode n, α_n is assigned according to the importance of minimizing the ratio of R_n to r_n, with the goal of minimizing τ_n. If mode 1 has a very large time constant, then priority should be given to minimizing its dwell time over that of mode 2 with a small time constant, since the system states decay much more slowly between the level sets of $\mathbf{X_1}$ than for those of $\mathbf{X_2}$. Therefore, α_1 should be bigger than α_2. As such, it is natural to choose $\alpha_n = \lambda_n$ for mode n.

Selecting γ_n presents a different challenge. The reason R_n must be limited is that $\mathbf{X_n}$ is not necessarily globally stable in the non-linear system. The exact region of attraction of an equilibrium point can be difficult to determine (21), but assessing the accuracy of mode n's globally stable linear approximation would provide a measure of how far the non-linear region of attraction might be trusted to extend, and this would motivate a choice of γ_n. If $\mathbf{A_n}\tilde{\mathbf{x}}$ is a close approximation to $\mathbf{f_n}(\mathbf{x})$, then mode n is more likely to be stable for states contained anywhere in B_n, and a larger R_n can be tolerated.

To evaluate the accuracy of the linear approximation at mode n, consider the expression for the error in the linear approximation of $\mathbf{f}(\mathbf{x})$, written

$$\mathbf{L_n}(\mathbf{x}) = \mathbf{A_n}\tilde{\mathbf{x}} - \mathbf{f}(\mathbf{x}) \tag{9}$$

The quality of the approximation relates to how quickly this term expands as $\|\tilde{\mathbf{x}}\|$ increases. One way to assess this is to pick a maximum bound M for the error and attempt to find the smallest ball centered on $\mathbf{X_n}$ such that, for some point $\mathbf{x}^*$ on the surface of the ball, $L_{n,i}(\mathbf{x}^*) = M$ for some i^{th} row of $\mathbf{L_n}(\mathbf{x})$.

This can be computationally expensive, so a more efficient algorithm is needed. This study implements a gradient ascent algorithm that, for each i, begins at $\mathbf{X_n}$, evaluates the gradient of $L_{n,i}(\mathbf{x})$, moves in the direction of maximum increase of $L_{n,i}(\mathbf{x})$, and evaluates $L_{n,i}(\mathbf{x})$ for the new point. Once a point $\mathbf{x}^*$ is found such that $L_{n,i}(\mathbf{x}^*) \geq M$, the algorithm returns the Euclidean distance from this point to $\mathbf{X_n}$. The minimum of these distances over i is chosen, and the inverse of this value is used as γ_n. Thus, both α_i and γ_i are obtained for

each $i \in \{1, 2, ..., N\}$ and (5) is well defined for minimization. If these weights ultimately produce undesirable dwell times, they can be adjusted. Example 2 demonstrates this. Figure 4 below presents the general proposed process in its entirety.

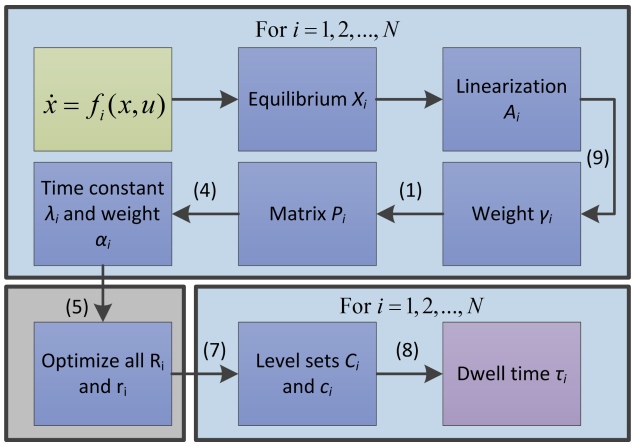

Figure 4. Algorithm flowchart

3.5. ILL-CONDITIONED SYSTEMS

Equation (6) shows that the semi-principal axes of the ellipsoids relate to the eigenvalues of **P**, which highlights a particular type of system as concerning. Consider a system in which the Lyapunov function for a mode contains a **P** matrix with extreme variation in its eigenvalues. In this case, the corresponding ellipsoid has some semi-principal axis lengths that are extremely long compared to others. Then the volume of the ball inscribed in this ellipsoid is small compared to the ellipsoid's volume, and the volume of the circumscribed ball is comparatively large. Such systems are common in areas such as electric machinery, in which there are both electrical and mechanical states.

Figure 5. An ill-conditioned mode

To demonstrate the issue, suppose that the continuous system states exist somewhere on the surface of B_n when the system is switched to mode n. Then the system states either intersect H_n, or they intersect some ellipsoid corresponding to a smaller level set of $V(\mathbf{x})$. The smallest level set that they might intersect is that which is inscribed in B_n, denoted T_n.

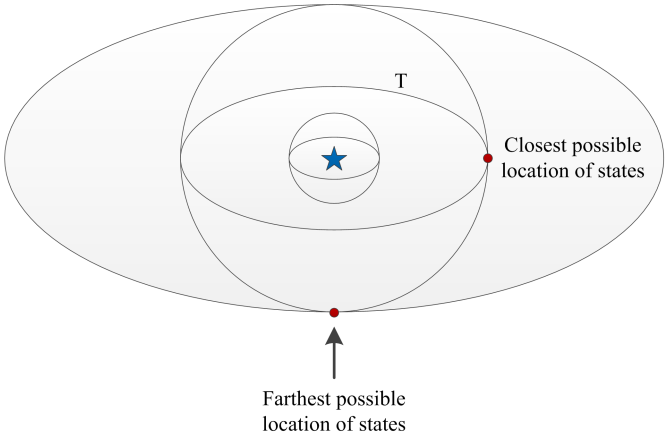

Figure 6. Ill-conditioned system with possible state locations and the T ellipsoid shown

Depending on where the states lie, then, they may need to travel all the way from H_n to h_n, or only from T_n to h_n. If the minimum dwell time is found by (8) and the states only have to travel from T_n to h_n, then τ_n could be much greater than the actual transition time. In this case, much time is wasted waiting on τ_n to pass. The level set corresponding to T_n can be found using (7) as

$$R_n^2 \lambda_{min}(\mathbf{P_n}) \tag{10}$$

This can be used to calculate the maximum possible time to decay from T_n to h_n as

$$-\lambda_n \ln\left(\frac{r_n^2 \lambda_{min}(\mathbf{P_n})}{R_n^2 \lambda_{min}(\mathbf{P_n})}\right) = -\lambda_n \ln\left(\frac{r_n^2}{R_n^2}\right) \tag{11}$$

Knowing the maximum possible time to decay from H_n to h_n from (8), these two transition times can be compared. A good measure of how ill-conditioned a system is given from the ratio of these two transition times:

$$K_n = \frac{\ln\left(\frac{r_n^2\lambda_{min}(\mathbf{P_n})}{R_n^2\lambda_{max}(\mathbf{P_n})}\right)}{\ln\left(\frac{r_n^2}{R_n^2}\right)} = 1 + \frac{\ln\left(\frac{\lambda_{min}(\mathbf{P_n})}{\lambda_{max}(\mathbf{P_n})}\right)}{\ln\left(\frac{r_n^2}{R_n^2}\right)} \tag{12}$$

The closer K_n is to 1, the better suited the system is to analysis in the present manner. The larger K_n is above 1 indicates the degree to which the system is ill-conditioned. For example, if $K_n = 2$, then in the worst-case scenario, twice as much time as necessary is waited when the system switches to mode n.

Analysis of (12) reveals something interesting: as r_n and R_n separate and $\frac{r_n^2}{R_n^2} \to 0$, $K_n \to 1$ even though $\tau_n \to \infty$. Similarly, as $\frac{r_n^2}{R_n^2} \to 1$, $K_n \to \infty$ while τ_n approaches its minimum value, given by

$$\tau_{n,min} = -\lambda_n \ln\left(\frac{\lambda_{min}(\mathbf{P_n})}{\lambda_{max}(\mathbf{P_n})}\right) \tag{13}$$

This shows that τ and K have an inverse relationship, which can be explicitly found:

$$K_n = \frac{\tau_n}{\tau_n + \lambda_n \ln\left(\frac{\lambda_{min}(\mathbf{P_n})}{\lambda_{max}(\mathbf{P_n})}\right)} \tag{14}$$

This helps to ease the concern that ill-conditioned systems raise. If K is very large, then τ should be small. Therefore, even if much time is wasted waiting relative to τ, this is likely small since τ is small. On the other hand, if τ is large, K should be small, so not very much time is comparatively wasted by waiting for τ to pass. In practice, one must consider both the τ and K values produced and decide whether or not they are feasible for the system in question.

4. EXAMPLES

4.1. BOOST CONVERTER

The procedure outlined in this study has been implemented in MATLAB. As an example, consider the boost converter below.

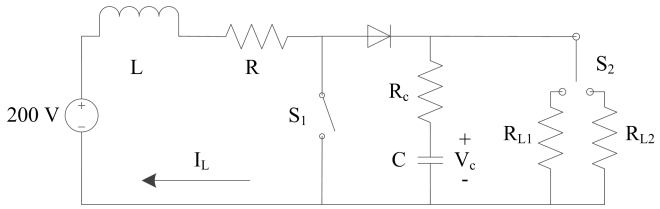

Figure 7. Diagram of boost converter

Suppose that S_1 switches with a duty cycle d, and that S_2 switches between R_{L1} and R_{L2}. The state space averaged model of this system is given below, where $u \in \{R_{L1}, R_{L2}\}$ and depends on the configuration of S_2.

$$\begin{pmatrix} \dot{I_L} \\ \dot{V_C} \end{pmatrix} = \begin{pmatrix} -\left(\frac{R_c R + u(dR_c + R)}{L(u+R_c)}\right) I_L - \left(\frac{du}{L(u+R_c)}\right) V_C \\ \\ \left(\frac{du}{C(u+R_c)}\right) I_L - \left(\frac{1}{C(u+R_c)}\right) V_C \end{pmatrix} \tag{15}$$

Suppose that $d = 0.5$, $R = R_c = 0.01\Omega$, $C = 0.12$mF, $L = 0.95$mH, $R_{L1} = 30\Omega$, and $R_{L2} = 500\Omega$. Let mode 1 be given by $u = R_{L1}$ and mode 2 by $u = R_{L2}$. Then the equilibrium points of the system are

$$\mathbf{X_1} = \begin{pmatrix} 26.6223\text{A} \\ 399.3345\text{V} \end{pmatrix}; \mathbf{X_2} = \begin{pmatrix} 1.5998\text{A} \\ 399.9600\text{V} \end{pmatrix}$$

The code also computes the ball sizes and minimum dwell times for each mode, respectively.

$$\begin{pmatrix} R_1 \\ r_1 \\ R_2 \\ r_2 \end{pmatrix} = \begin{pmatrix} 26.8845 \\ 0.6173 \\ 25.6476 \\ 1.8542 \end{pmatrix}; \begin{pmatrix} \tau_1 \\ \tau_2 \end{pmatrix} = \begin{pmatrix} 0.1465\text{s} \\ 1.0058\text{s} \end{pmatrix}$$

An illustration of the operating points and balls for this system is given below.

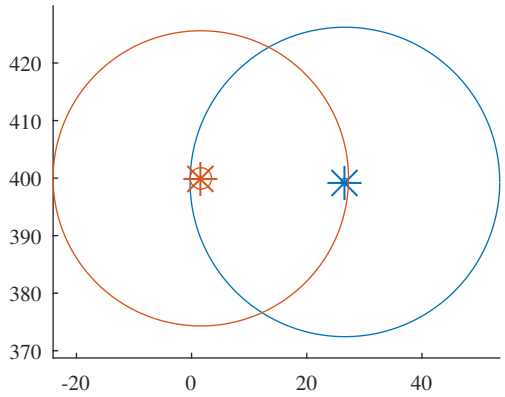

Figure 8. Stable operating points and balls for the boost converter system

4.2. INDUCTION MACHINE

As a non-linear example, consider a 4-pole, squirrel-cage induction motor driven by a variable frequency drive (VFD). The state space model in the *dq* reference frame has five states, which are the stator *dq* currents, rotor *dq* currents, and rotor electrical speed. The state vector is

$$\mathbf{X} = \begin{pmatrix} I_{qs} \\ I_{ds} \\ I_{qr} \\ I_{dr} \\ \omega_r \end{pmatrix}$$

$$\begin{pmatrix} \dot{I_{qs}} \\ \dot{I_{ds}} \\ \dot{I_{qr}} \\ \dot{I_{dr}} \\ \dot{\omega_r} \end{pmatrix} = \begin{pmatrix} \frac{-R_s I_{qs} - 2\pi f L_{ss} I_{ds} - 2\pi f L_m I_{dr}}{L_{ss}} \\ -\frac{L_m(\frac{2\pi f L_m^2 I_{dr} + L_m R_s I_{qs} - L_m}{L_{ss}} + I_{ds}\omega_r L_m - R_r I_{qr} - 2\pi f L_{rr} I_{dr} + I_{dr}\omega_r L_{rr})}{L_{rr} - L_m^2} \\ \frac{V_{ds} + 2\pi f L_{ss} I_{qs} - R_s I_{ds} + 2\pi f L_m I_{qr}}{L_{ss}} \\ -\frac{L_m(-I_{qs}\omega_r L_m + \frac{L_m R_s I_{ds} - L_m V_{ds} - 2\pi f L_m^2 I_{qr}}{L_{ss}} + L_{rr} I_{qr} 2\pi f - I_{qr}\omega_r L_{rr} - R_r I_{dr})}{L_{rr} - L_m^2} \\ \frac{L_m(\frac{2\pi f L_m^2 I_{dr} + L_m R_s I_{qs} - L_m}{L_{ss}} + I_{ds}\omega_r L_m - R_r I_{qr} - 2\pi f L_{rr} I_{dr} + I_{dr}\omega_r L_{rr})}{L_{rr} - L_m^2} \\ \frac{L_m(-I_{qs}\omega_r L_m + \frac{L_m R_s I_{ds} - L_m V_{ds} - 2\pi f L_m^2 I_{qr}}{L_{ss}} + L_{rr} I_{qr} 2\pi f - I_{qr}\omega_r L_{rr} - R_r I_{dr})}{L_{rr} - L_m^2} \\ \frac{6L_m}{J}(I_{qs} I_{dr} - I_{ds} I_{qr}) - \frac{2T_L}{J} - \frac{\omega_r B}{J} \end{pmatrix} \tag{16}$$

The inputs to the system are the line-to-neutral source voltage V_{ds} and source frequency f, which are switched by the VFD. Since the rotor windings are shorted, the rotor direct and quadrature voltages are both zero. Also, the stator quadrature voltage is assumed zero to simplify the model. So the input vector is

$$\mathbf{U} = \begin{pmatrix} V_{ds} \\ f \end{pmatrix}$$

The state-space model of this system can be seen in (16) and has been adapted from (23; 24). Table 1 defines each term and provides the numerical values used in this example. These values are taken from a Baldor M3115T, 1 hp, 230 V, 60 Hz, 4-pole induction motor.

Consider three different VFD inputs:

$$\mathbf{U_1} = \begin{pmatrix} 100V \\ 50Hz \end{pmatrix}; \mathbf{U_2} = \begin{pmatrix} 110V \\ 55Hz \end{pmatrix}; \mathbf{U_3} = \begin{pmatrix} 120V \\ 60Hz \end{pmatrix}$$

These inputs result in the stable operating points

Table 1. Induction motor model symbols and values

Term	Quantity Represented	Numerical Value
R_s	Steinmetz stator resistance	5.18 Ω
R_r	Referred rotor resistance	4.3 Ω
L_m	Magnetizing reactance	239 mH
L_{ss}	Sum of stator reactance and L_m	251 mH
L_{rr}	Sum of rotor reactance and L_m	257 mH
T_L	Load torque on machine	1 N·m
J	Moment of inertia of rotor and load	0.1 kg·m^2
B	Coefficient of kinetic friction of rotor	0.001

$$\mathbf{X_1} = \begin{pmatrix} -1.3032\text{A} \\ 1.3902\text{A} \\ 0.1167\text{A} \\ -1.3851\text{A} \\ 355.83\text{rad/s} \end{pmatrix}; \mathbf{X_2} = \begin{pmatrix} -1.2885\text{A} \\ 1.3857\text{A} \\ 0.1082\text{A} \\ -1.3745\text{A} \\ 324.48\text{rad/s} \end{pmatrix}$$

$$\mathbf{X_3} = \begin{pmatrix} -1.2716\text{A} \\ 1.3836\text{A} \\ 0.0991\text{A} \\ -1.3653\text{A} \\ 293.08\text{rad/s} \end{pmatrix},$$

and the resulting ball radii and dwell times are

$$\begin{pmatrix} R_1 \\ r_1 \\ R_2 \\ r_2 \\ R_3 \\ r_3 \end{pmatrix} = \begin{pmatrix} 63.3775 \\ 0.5579 \\ 32.0243 \\ 31.9111 \\ 63.3129 \\ 0.6225 \end{pmatrix}; \begin{pmatrix} \tau_1 \\ \tau_2 \\ \tau_3 \end{pmatrix} = \begin{pmatrix} 25.4957\text{s} \\ 10.5922\text{s} \\ 24.2170\text{s} \end{pmatrix}.$$

In this case, the ratio of R_n to r_n is typically large, and this results in somewhat large dwell times. If desired, the α weights of section 3.4 can be increased to reduce the dwell times. Increasing each α weight by a factor of 10,000 gives

$$\begin{pmatrix} R_1 \\ r_1 \\ R_2 \\ r_2 \\ R_3 \\ r_3 \end{pmatrix} = \begin{pmatrix} 121.4222 \\ 58.7157 \\ 90.0689 \\ 90.0689 \\ 121.4707 \\ 58.6672 \end{pmatrix}; \begin{pmatrix} \tau_1 \\ \tau_2 \\ \tau_3 \end{pmatrix} = \begin{pmatrix} 13.0303\text{s} \\ 10.5814\text{s} \\ 12.5241\text{s} \end{pmatrix}.$$

Though the radii are larger, they are not unreasonably so, and the dwell times are roughly halved by this procedure. This demonstrates how experimenting with the α and γ weights can help accommodate the system at hand.

ACKNOWLEDGEMENTS

Work supported by National Science Foundation Award 1505610.

REFERENCES

[1] D. Liberzon, *Switching in Systems and Control*. New York, NY: Birkhäuser, 2003.

[2] J. P. Hespanha and A. S. Morse, "Stability of switched systems with average dwell time," in *38th Conference on Decision and Control*, 1999.

[3] D. Liberzon and A. S. Morse, "Basic problems in stability and design of switched systems," *IEEE Control Systems Magazine*, vol. 19, October 1999.

[4] X. Gao, D. Liberzon, J. Liu, and T. Basar, "Unified stability criteria for slowly time-varying and switched linear systems," *Automatica*, 2018.

[5] X. Zhao, L. Zhang, P. Shi, and M. Liu, "Stability and stabilization of switched linear systems with mode-dependent average dwell time," *IEEE Transactions on Automatic Control*, vol. 57, pp. 1809–1815, July 2012.

[6] X. Zhao, S. Yin, H. Li, and B. Niu, "Switching stabilization for a class of slowly switched systems," *IEEE Transactions on Automatic Control*, vol. 60, pp. 221–226, 2015.

[7] M. S. Branicky, "Multiple lyapunov functions and other analysis tools for switched and hybrid systems," *IEEE Transactions on Automatic Control*, vol. 43, pp. 475–482, April 1998.

[8] J. C. Geromel and P. Colaneri, "Stability and stabilization of continuous-time switched linear systems," *IEEE Control Systems Magazine*, vol. 45, no. 5, pp. 1915–1930, 2006.

[9] A. Kundu and D. Chatterjee, "Stabilizing switching signals for switched systems," *IEEE Transactions on Automatic Control*, vol. 60, pp. 882–888, March 2015.

[10] J. Lee and G. E. Dullerud, "Uniformly stabilizing sets of switching sequences for switched linear systems," *IEEE Transactions on Automatic Control*, vol. 52, pp. 868–874, May 2007.

[11] R. A. Decarlo, M. S. Branicky, S. Pettersson, and B. Lennartson, "Perspectives and results on the stability and stabilizability of hybrid systems," *Proceedings of the IEEE*, vol. 88, no. 7, pp. 1069–1082, July 2000.

[12] G. Davrazos and N. T. Koussoulas, "A review of stability results for switched and hybrid systems," in *Proc. 9th Mediterranean Conference on Control and Automation*, 2001.

[13] H. Lin and P. J. Antsaklis, "Stability and stabilizability of switched linear systems: A survey of recent results," *IEEE Transactions on Automatic Control*, vol. 54, pp. 308–322, February 2009.

[14] X. Xu and G. Zhai, "Practical stability and stabilization of hybrid and switched systems," *IEEE Transactions on Automatic Control*, vol. 50, no. 11, pp. 1897–1903, Nov 2005.

[15] G. Zhai and A. N. Michel, "Generalized practical stability analysis of discontinuous dynamical systems," in *42nd IEEE International Conference on Decision and Control (IEEE Cat. No.03CH37475)*, vol. 2, Dec 2003, pp. 1663–1668 Vol.2.

[16] T. Alpcan and T. Basar, "A stability result for switched systems with multiple equilibria," *Dynamics of Continuous, Discrete, and Impulsive Systems*, vol. 17, pp. 949–958, May 2010.

[17] F. Blanchini, D. Casagrande, and S. Miani, "Modal and transition dwell time computation in switching systems: A set-theoretic approach," *Automatica*, vol. 46, pp. 1477–1482, July 2010.

[18] R. Kuiava, R. A. Ramos, H. R. Pota, and L. F. C. Alberto, "Practical stability of continuous-time switched systems without a common equilibria and governed by a time-dependent switching signal," in *2011 9th IEEE International Conference on Control and Automation (ICCA)*, Dec 2011, pp. 1156–1161.

[19] R. Kuiava, R. A. Ramos, L. F. C. Alberto, and H. R. Pota, "Practical stability assessement of distributed synchronous generators under load variations," in *2013 IEEE International Symposium on Circuits and Systems (ISCAS2013)*, May 2013, pp. 457–460.

[20] G. Chesi, P. Colaneri, J. C. Geromel, and R. Middleton, "Computing upper-bounds of the minimum dwell time of linear switched systems via homogeneous polynomial lyapunov functions," in *American Control Conference Proc.*, 2010, pp. 2487–2492.

[21] H. K. Khalil, *Nonlinear Systems*. Upper Saddle River, NJ: Prentice Hall, 2001.

[22] M. Caramia and P. Dell'Olmo, *Multi-objective Management in Freight Logistics*. London, UK: Springer-Verlag, 2008.

[23] R. Krishnan, *Electric Motor Drives: Modeling, Analysis, and Control*. Upper Saddle River, NJ: Prentice Hall, 2001.

[24] P. C. Krause, O. Wasynczuk, and S. D. Sudhoff, *Analysis of Electric Machinery and Drive Systems*, 2nd ed. Piscataway, NJ: IEEE Press, 2002.

[25] M. Rasheduzzaman, J. A. Mueller, and J. W. Kimball, "An accurate small-signal model of inverter-dominated islanded microgrids using dq reference frame," *IEEE Journal of Emerging and Selected Topics in Power Electronics*, vol. 2, December 2014.

[26] Z. Gajić and M. T. J. Qureshi, *Lyapunov Matrix Equation in System Stability and Control*. San Diego, CA: Academic Press, 1995.

[27] H. G. Kwatny and G. L. Blankenship, *Nonlinear Control and Analytical Mechanics*. New York, NY: Birkhäuser, 2000.

II. PRACTICAL DWELL TIMES FOR SWITCHED SYSTEMS WITH MULTIPLE OPERATING POINTS FOR MICROGRID STABILITY

W. R. St. Pierre, B. Zhou, and J. W. Kimball

Department of Electrical Engineering

Missouri University of Science and Technology

Rolla, Missouri 65409–0050

Tel: 573–341–6622, Fax: 573–341–4115

Email: wrsthf@mst.edu

ABSTRACT

This paper presents a practical algorithm for obtaining dwell times that guarantee the stability of switched systems with multiple stable operating points. This method is implementable for an arbitrary switched system with potentially large numbers of states and subsystems. After a brief relevant background, the approach is developed and its stability shown. An analysis of the process is included, and simulations are performed on a boost converter, microgrid system, and seven bus grid model to demonstrate its effectiveness.

Keywords: Switched systems, nonlinear systems, Lyapunov

1. INTRODUCTION

Switched systems are pervasive in engineering applications, inspiring much investigation into their stability. These systems switch their dynamics over time within a finite set of discrete modes. Traditional techniques can assess the stability of each individual subsystem, but they do not assure stability of the overall system under switching, because certain switching signals may force the state trajectories into unacceptable regions.

Many results exist to show stability under switching for systems whose modes all converge to a shared stable operating point, as might occur when several controllers are needed to produce a single desired behavior. In this vein, (1) presents the calculation for a single minimum dwell time which, if elapsed between all consecutive switching actions, guarantees stability under switching.

Also relevant is the concept of average dwell time, which ensures stability when switching is limited on the average (2; 3). One technique produces mode-dependent average dwell times, which require that the number of switches to a particular mode is limited on the average of its total active time, and these are used to show global uniform exponential stability of linear switched systems (5; 6). More recently, (4) generalized results on the stability of slowly time-varying systems to produce average dwell times for switched linear systems.

Other approaches to switched system stability exist as well, such as the Lyapunov techniques discussed in (7; 11). Stability can be deduced if a Lyapunov function is found that is common to all subsystems. When this not possible, multiple Lyapunov functions can be used to show asymptotic stability for certain switching signals. Also, (10) develops processes to identify the set of all switching signals that grant uniform stability. Likewise, (9) uses multiple Lyapunov-like functions and switching frequency notions to expand the set of known stabilizing switching signals beyond those rendered by minimum or average dwell time methods. However, all above approaches are applicable only to systems with a single operating point. More methods for such systems are surveyed in (12; 13).

In practice, many switched systems contain modes with their own distinct operating points. Some work has been done to generalize the above results to such systems. One useful concept is that of *practical stability*, as introduced in (14; 15). Informally, a switched system is practically stable under a given switching signal if its states remain in a predefined bounded set as long as the initial states are within a subset of this set. Most results for switched systems with multiple operating points achieve something similar to practical

stability. Theorems are derived in (14) for assessing whether a switched system is practically stabilizable, and the designs of two switching laws that can practically stabilize a system are provided. This contribution is for the case in which the switching signal is controlled.

When control of the switching sequence does not exist, switching actions can be monitored to ensure compliance with stabilizing conditions, such as dwell times. For example, (16) outlines a method to procure a universal minimum dwell time that guarantees trajectory convergence to a superset of the multiple system equilibria. However, the result is somewhat analytical and difficult to apply to real world systems that may contain hundreds of modes and equilibria, as is common in power systems. Global exponential stability of each operating point is also assumed, which limits the reach of the result.

Another method uses set theory to find modal dwell times (where the necessary dwell time depends on the active subsystem) that ensure that states remain restricted to a finite region about the equilibria (17). These dwell times can limit the states to a known admissible region (if this region is large enough). However, the sets involved can be hard to compute, especially for high order systems. Because of this, the authors suggest computing less ideal Lyapunov level sets for each mode that lie within the admissible region, and using these for more conservative dwell times. However, it can be difficult to find these functions, and yet more difficult to verify that they are contained in an arbitrary region.

An application focused method is presented in (18), which formulates a minimum dwell time for practical stability over finite time intervals. One major drawback is that the process is not applied to the perpetual time interval case, which is necessary for guaranteeing sustained stability. It is also not always possible to meet the conditions of the relevant theorems. The authors extend the results to a small power grid example in (19), which emphasizes the applied intention.

This paper presents an algorithm for determining modal dwell times for switched system stability that is similar in spirit to the work in (16) and (17), but is more practical for complex systems. The achieved stability is very similar to the practical stability of

(18), and will show that states are bounded to a finite set about the equilibria if certain initial conditions are met. However, the stability will be granted perpetually, and the dwell times will not depend on a considered finite time interval. This procedure is intended to be easily applicable to many physical switched systems, and is especially developed for power systems as in (19). Several examples are drawn from power applications.

2. BACKGROUND AND MOTIVATION

2.1. PRELIMINARIES

Consider a family of nonlinear functions $F = \{f_j(x,u) : j \in J\}$ where J is an indexing set. Define the switched system $\mathcal{S}$ as

$$\dot{\mathbf{x}} = \mathbf{f}_{\sigma(\mathbf{t})}(\mathbf{x}, \mathbf{u}), \tag{1}$$

where $x \in \mathbb{R}^n$ and switching signal $\sigma(t)$ is a piecewise constant function defined on (t_0, ∞) that takes its values from J and indicates the system dynamics (or mode) at time t. This structure characterizes a switched system, and each discrete jump in $\sigma(t)$ between two elements of j is known as a switching event.

For two switching events occuring at t_i and t_{i+1}, the dwell time between these events is $t_{i+1} - t_i$. This paper imposes modal dwell time restrictions on $\sigma(t)$ for each mode of $\mathcal{S}$. If τ_j is a modal dwell time for mode j, then $t_{i+1} - t_i \geq \tau_j$ for every t_i such that $\sigma(t_i^+) = j$. In other words, τ_j is the minimum amount of time that must pass after switching to mode j before switching to another mode.

The type of stability achieved will be similar to the practical stability defined in (15), so it is worth restating the formal definition here. The below definition differs only in that it is formulated for an infinite time interval.

Definition 1

The switched system (1) is *practically stable* with respect to $(\Omega_1, \Omega_2, \sigma(t))$, where Ω_1, $\Omega_2 \subset \mathbb{R}^n$, $\Omega_1 \subset \Omega_2$, if $x(t_0) \in \Omega_1$ implies $x(t) \in \Omega_2$ for all $t \in [t_0, \infty)$.

This paper also makes use of an upper bound on convergence rates of Lyapunov functions for linear systems. If

$$\dot{\mathbf{x}} = \mathbf{A}\mathbf{x} \tag{2}$$

is a stable linear system, then a Lyapunov function for the system can be obtained as $V(\mathbf{x}) = \mathbf{x}^\mathbf{T}\mathbf{P}\mathbf{x}$ using the Lyapunov equation $\mathbf{A}^\mathbf{T}\mathbf{P} + \mathbf{P}\mathbf{A} = -\mathbf{Q}$ where $\mathbf{P}$ and $\mathbf{Q}$ are symmetric and positive definite matrices. This also grants that $\dot{V}(\mathbf{x}) = -\mathbf{x}^\mathbf{T}\mathbf{Q}\mathbf{x}$. Since $V(\mathbf{x}) \leq \lambda_{max}(\mathbf{P})\|x\|^2$ where $\lambda_{max}(\mathbf{P})$ is the largest eigenvalue of $\mathbf{P}$, it can be shown that

$$\dot{V}(\mathbf{x}) = -\mathbf{x}^\mathbf{T}\mathbf{Q}\mathbf{x} \leq -\lambda_{min}(\mathbf{Q})\|x\|^2 \leq -\frac{\lambda_{min}(\mathbf{Q})}{\lambda_{max}(\mathbf{P})}V(\mathbf{x}). \tag{3}$$

The solution to this ordinary differential equation is

$$V(\mathbf{x}) \leq V_0 \exp\left(-\frac{\lambda_{min}(\mathbf{Q})}{\lambda_{max}(\mathbf{P})}t\right), \tag{4}$$

which gives $\lambda = \frac{\lambda_{max}(\mathbf{P})}{\lambda_{min}(\mathbf{Q})}$ as a worst-case scenario time constant for the decay of the Lyapunov expression.

2.2. MOTIVATING ANALYSIS OF UNSTABLE SWITCHING

As both motivation and a useful analysis tool, a switching law is described here that can cause instability in a switched system. This can indicate the susceptibility of the system to a switching attack.

Consider two arbitrary linear modes i and j, with Lyapunov functions V_i and V_j. To target instability, the system can be switched between these two modes whenever one subsystem's Lyapunov function is maximized while the dynamics are governed by the other. Suppose the currently active subsystem is j. The system should be switched from j to i when

$$\frac{dV_i}{dt} = \frac{dV_i}{d\tilde{\mathbf{x}}_j}\frac{d\tilde{\mathbf{x}}_j}{dt} = (\tilde{\mathbf{x}}_i^T\mathbf{P}_i)(\mathbf{A}_j\tilde{\mathbf{x}}_j) = 0, \tag{5}$$

so that V_i is at a critical point. To ensure this is a maximum, the second time derivative must be negative. This condition is

$$\frac{d(\tilde{\mathbf{x}}_i^T\mathbf{P}_i)(\mathbf{A}_j\tilde{\mathbf{x}}_j)}{dt} = (\tilde{\mathbf{x}}_i^T\mathbf{P}_i\mathbf{A}_j + \tilde{\mathbf{x}}_j^T\mathbf{A}_j^T\mathbf{P}_i^T)\mathbf{A}_j\tilde{\mathbf{x}}_j < 0. \tag{6}$$

The system can be switched back to mode j by the same rule, and so on. This is not guaranteed to cause instability, but it is often effective, as Example 6.1 shows.

3. MAIN RESULT

The proposed method for obtaining dwell times that ensure system stability is described in this section. As mentioned, it has some similarities to (16) and (17), but is designed to be more computationally feasible as an algorithm. A thorough comparison is made in Section 4.4.

Consider a system of the form (1). To enable a practical analysis, each subsystem is linearized about its stable operating point. Let $\mathbf{X_j}$ denote the equilibrium of mode j. Then a linear approximation of the mode is given by

$$\dot{\tilde{\mathbf{x}}} = \mathbf{A_j}\tilde{\mathbf{x}}_\mathbf{j}, \tag{7}$$

where $\tilde{\mathbf{x}}_\mathbf{j} = \mathbf{x} - \mathbf{X}_\mathbf{j}$ shifts the equilibrium point of the linearized system to the origin, and $\mathbf{A}_\mathbf{j}$ is the Jacobian of the subsystem evaluated at $\mathbf{X}_\mathbf{j}$ and $\mathbf{u}$. Suppose that each linearized subsystem is stable. Then Lyapunov's Indirect Method grants that each nonlinear subsystem is stable for some (possibly small) neighborhood about its equilibrium. Next, a Lyapunov function V_j is determined for each $j \in J$ as outlined in section 2 with corresponding time constant λ_j. As long as $\mathbf{x}$ is sufficiently close to $\mathbf{X}_\mathbf{j}$ in mode j, it will converge at a rate bounded above by the slowest possible decay rate of V_j, which is λ_j. If an η is known such that $\dot{V}_j(\mathbf{x}) \leq -\eta V(\mathbf{x})$ and $\eta > \frac{\lambda_{min}(\mathbf{Q})}{\lambda_{max}(\mathbf{P})}$, λ_j can be taken as $\frac{1}{\eta}$ instead.

A level set of $V(\mathbf{x})$ of size C is $\{\mathbf{x} : V(\mathbf{x}) = C\}$. For Lyapunov functions of the form $V(\mathbf{x}) = \mathbf{x}^\mathbf{T}\mathbf{P}\mathbf{x}$, these level sets are ellipsoids centered on their respective operating points. The algorithm proposed here selects two such level sets for each system mode in a manner soon to be introduced. Call the larger of these H of size C and the smaller h of size c. Let the ball inscribed in H be called B with radius R, and let the ball circumscribed about h be called b with radius r. This will simplify future operations.

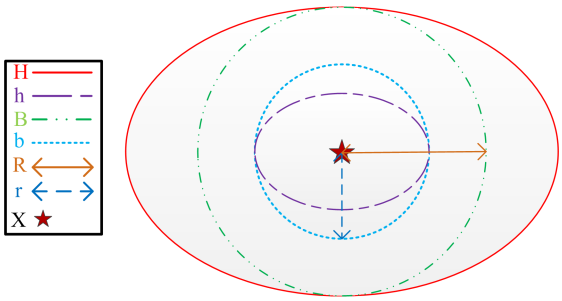

Figure 1. Depiction of a mode with associated objects

For modes j_1 and j_2, it is required that $b_{j1} \subseteq B_{j2}$ for all $j_1, j_2 \in J$. This provides the structure to prove the critical result, which states that (1) is practically stable for $\Omega_1 = \cup_j b_j$, $\Omega_2 = \cup_j H_j$, and $\sigma(t)$ satisfying a modal dwell time constraint.

Theorem 3.1. *Consider the switched system (1) with $\sigma(t)$ obeying modal dwell times*

$$\tau_j = -\lambda_j \ln\left(\frac{c_j}{C_j}\right) \tag{8}$$

for each $j \in J$. Let t_i denote a switching time for $i \in \mathbb{N}$. If $\mathbf{x}(t_0) \in b_{\sigma(t_0^-)}$, then $\mathbf{x}(t) \in \cup_j H_j$ for all $t \geq t_0$.

Proof. If $\mathbf{x}(t_0) \in b_{\sigma(t_0^-)}$, then $\mathbf{x}(t_0) \in H_{\sigma(t_0^+)}$ because $b_{\sigma(t_0^-)} \subseteq B_{\sigma(t_0^+)} \subseteq H_{\sigma(t_0^+)}$. So $V_{\sigma(t_0^+)}(t_0) \leq C_{\sigma(t_0^+)}$, and $\mathbf{x}(t) \in H_{\sigma(t_0^+)}$ for all $t \in [t_0, t_1)$, since $\dot{V}_{\sigma(t_0^+)}$ is negative definite. Thus $\mathbf{x}(t) \in \cup_J H_j$ for $t \in (t_0, t_1)$. Also,

$$V_{\sigma(t_0^+)}(t_1) \leq V_{\sigma(t_0^+)}(t_0) e^{-\frac{t_1 - t_0}{\lambda_{\sigma(t_0^+)}}}$$

$$\leq V_{\sigma(t_0^+)}(t_0) e^{-\frac{\tau_{\sigma(t_0^+)}}{\lambda_{\sigma(t_0^+)}}} = V_{\sigma(t_0^+)}(t_0) \frac{c_{\sigma(t_0^+)}}{C_{\sigma(t_0^+)}} \leq c_{\sigma(t_0^+)},$$

so $\mathbf{x}(t_1) \in h_{\sigma(t_1^-)}$, which implies that $\mathbf{x}(t_1) \in \cup_J H_j$ and $\mathbf{x}(t_1) \in b_{\sigma(t_1^-)}$. By induction, $\mathbf{x}(t) \in \cup_j H_j$ for all $t \geq t_0$. □

Remark 1. *If certain transitions between system modes are not possible, then the requirement that $b_{j1} \subseteq B_{j2}$ for all $j_1, j_2 \in J$ can be relaxed. If the system cannot switch from j_1 to j_2, then B_{j_2} needn't contain b_{j_1} and the above proof will still hold because of the transition restriction. Examples 6.1 and 6.3 explore relaxation of this requirement.*

4. PRACTICAL APPLICATION

Stability has been validated, but many aspects of the procedure remain open to choice. The next sections describe how to practically select balls B_j and b_j for all $j \in J$ and calculate the values of C_j and c_j from R_j and r_j in order to obtain τ_j by the formula in equation 8.

4.1. SELECTING BALL SIZES

Fig. 2 illustrates a scenario with four modes and one set of choices for their corresponding balls. Two considerations should influence the selection of B_j and b_j for mode j. First, the nonlinear subsystems are only guaranteed locally stable by the Lyapunov analysis.

Therefore the size of B_j should be as small as possible so that states are contained as close as possible to $\mathbf{X_j}$. Also, the dwell time τ_j is dependent on the ratio $\frac{c_j}{C_j}$, which is directly proportional to $\frac{r_j}{R_j}$. Minimizing $\frac{R_j}{r_j}$ makes this dwell time as small as possible.

Therefore, it is desirable to minimize both $\frac{R_j}{r_j}$ and R_j for all $j \in J$ while maintaining the original condition that $b_{j1} \subseteq B_{j2}$ for all $j_1, j_2 \in J$. This is a constrained multi-objective optimization problem, and a Pareto optimal solution can be obtained by minimizing a weighted sum of the objectives, written

$$F = \sum_{i=1}^{N} \alpha_i \frac{R_i}{r_i} + \gamma_i R_i \tag{9}$$

for a system with N modes. The α_i and γ_i weight coefficients have some flexibility and can be tuned to achieve desired dwell times or ball sizes, but one way to initially select them is to scale them to the relative importance of minimizing their terms over the others.

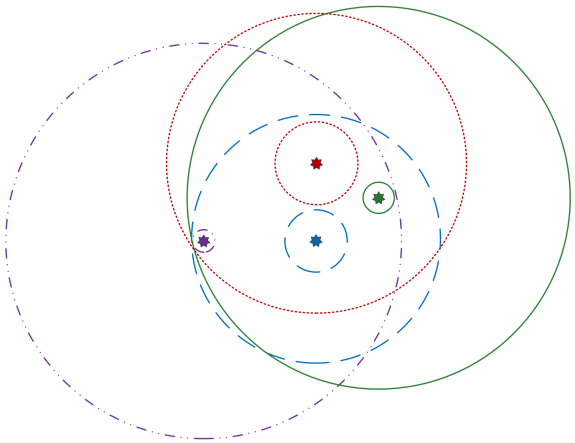

Figure 2. Example collection of four modes with balls

Increasing α_j is related to reducing τ_j, which is directly proportional to time constant λ_j. Modes with large time constants will likely have large dwell times, so reducing these is prioritized over reducing the comparatively small dwell times of other modes. This gives $\alpha_j = \lambda_j$ as a natural choice, since a greater λ implies a greater minimization priority.

The role of γ_j is to limit R_j so that B_j is contained in the region about $\mathbf{X_j}$ for which local stability holds. In application, any practical knowledge of system behavior can help an engineer to evaluate whether B_j is in a stable region for each j, but this cannot be guaranteed in general. However, confidence increases if the tolerance in R_j depends on the accuracy of the linear approximation of about $\mathbf{X_j}$. For a highly nonlinear mode with a poor approximation, R_j should be restricted as much as possible, as local stability cannot be trusted to extend very far.

One way to evaluate the quality of the approximation about $\mathbf{X_j}$ is to consider its error, written

$$\mathbf{E_j}(\mathbf{x}) = \mathbf{A_j}\tilde{\mathbf{x}}_\mathbf{j} - \mathbf{f_j}(\mathbf{x}). \tag{10}$$

The accuracy of the approximation is determined by how quickly $\mathbf{E_j}$ increases with $\|\tilde{\mathbf{x}}_\mathbf{j}\|$. For an arbitrary bound E_M, determining the smallest $\|\tilde{\mathbf{x}}_\mathbf{j}\|$ such that $\mathbf{E_j}(\mathbf{x}) = E_M$ (call this $\tilde{x}_{M,j}$) provides a serviceable measure of the quality of the linear approximation of subsystem j compared to the others. This value can be expensive to compute exactly, but a gradient descent algorithm performs well enough while offering an efficient solution. Since a small $\tilde{x}_{M,j}$ implies a poor approximation and thus a high minimization priority, $\gamma_j = \frac{1}{\tilde{x}_{M,j}}$ is a suitable choice.

4.2. CALCULATION OF DWELL TIMES

Determining τ_j from equation 8 requires knowledge of C_j and c_j. To find these, see that for $V_j(\tilde{\mathbf{x}}) = \tilde{\mathbf{x}}^\mathbf{T}\mathbf{P_j}\tilde{\mathbf{x}}$ there exists a coordinate rotation $\mathbf{y} = \mathbf{M_j}\tilde{\mathbf{x}}$ for an orthogonal $\mathbf{M_j}$ such that $V_j(\mathbf{y}) = \mathbf{y}^\mathbf{T}\mathbf{L_j}\mathbf{y}$ where $\mathbf{L_j}$ is diagonal, since $\mathbf{P_j}$ is symmetric. This gives the largest and smallest semi-principal axis lengths of the ellipsoid $V(\mathbf{y}) = C$ as

$$Z = \sqrt{\frac{C}{\lambda_{min}(\mathbf{P})}} \tag{11}$$

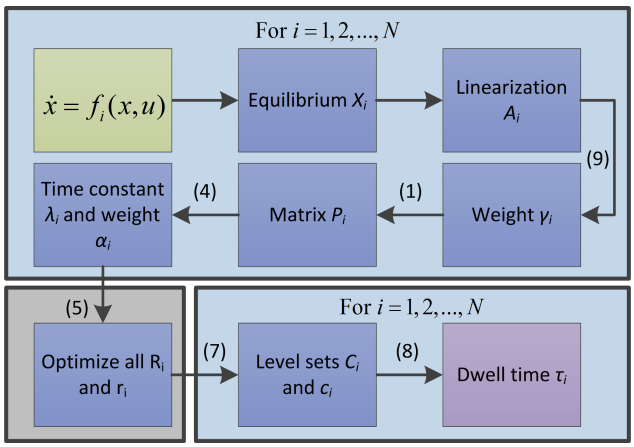

Figure 3. Illustration of procedure

and

$$z = \sqrt{\frac{C}{\lambda_{max}(\mathbf{P})}} \tag{12}$$

respectively. Since B_j is inscribed in H_j and b_j is circumscribed about h_j, $R_j = z_{H_j}$ and $r_j = Z_{h_j}$. Equations 11 and 12 then give C_j and c_j as

$$C_j = R_j^2 \lambda_{max}(\mathbf{P_j}), \tag{13}$$

$$c_j = r_j^2 \lambda_{min}(\mathbf{P_j}), \tag{14}$$

and τ_j can be found from equation (8). If unfavorable dwell times are produced after running this procedure for each $j \in J$, the α weights may be adjusted in an effort to improve them. Figure 3 graphically depicts the algorithm developed in this paper.

4.3. ILL-CONDITIONED SYSTEMS

In some systems, certain states converge much faster than others. This is commonly the case in electric machinery, as mechanical states are much slower than electrical.When this occurs, Lyapunov functions of the linearized system have more extreme variation in the eigenvalues of their **P** matrices, which causes greater skew in their elliptical level sets. These are called ill-conditioned systems, and they can yield dwell times that are too conservative.

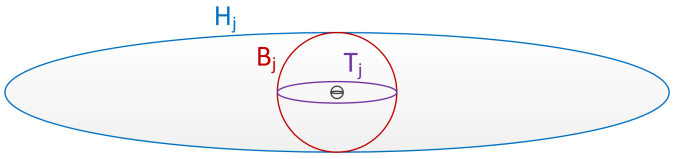

Figure 4. An ill-conditioned mode

Consider the two dimensional ill-conditioned switched system illustrated in Figure 4 and suppose it is switched to mode j at $t = 0$. Assuming the worst case, $\tilde{\mathbf{x}}_\mathbf{j}(0)$ is on the surface of B_j. In this case, if $\tilde{\mathbf{x}}_\mathbf{j}(0)$ is in the direction along the minor axis of H_j, then it is on the surface of H_j, and the dwell time given by (8) is appropriate. If, however, it is along the major axis of H_j, it is on the surface of a much smaller level set of V_j, which is labeled T_j in the figure. In this case the required dwell time would be much smaller, because the C_j term in (8) could be replaced by the much smaller magnitude of T_j. The more ill-conditioned the system, the greater this difference will be, and the dwell time given by (8) may be far too conservative in these cases.

Mathematically, the magnitude of T_j can be found by techniques in section 4.2 to be $R_j^2 \lambda_{min}(\mathbf{P_j})$. Substitution into (8) gives the minimum necessary dwell time as

$$\tau_{j,min} = -\lambda_j \ln\left(\frac{r_j^2 \lambda_{min}(\mathbf{P_j})}{R_j^2 \lambda_{min}(\mathbf{P_j})}\right) = -\lambda_j \ln\left(\frac{r_j^2}{R_j^2}\right). \tag{15}$$

The ratio of $\tau_{j,min}$ to the dwell time by (8) provides a measure of how ill-conditioned a subsystem is, which can be written

$$K_j = \frac{\ln\left(\frac{r_j^2 \lambda_{min}(\mathbf{P_j})}{R_j^2 \lambda_{max}(\mathbf{P_j})}\right)}{\ln\left(\frac{r_j^2}{R_j^2}\right)} = 1 + \frac{\ln\left(\frac{\lambda_{min}(\mathbf{P_j})}{\lambda_{max}(\mathbf{P_j})}\right)}{\ln\left(\frac{r_j^2}{R_j^2}\right)}. \tag{16}$$

A greater K_j implies a greater degree of ill-condition in subsystem j. For example, if $K_j = 2$ and system is switches to mode j when $\tilde{\mathbf{x}}_\mathbf{j}(0)$ is on the surface of T_j, the dwell time by (8) causes twice as much time than necessary to pass before more switching can occur.

Despite this, (16) allays concern to some extent, because as $\frac{r_j^2}{R_j^2} \to 0$, $K_j \to 1$ (even though $\tau_j \to \infty$), and as $\frac{r_j^2}{R_j^2} \to 1$, $K_j \to \infty$, but τ_j approaches its lower bound of

$$\underline{\tau_j} = -\lambda_j \ln\left(\frac{\lambda_{min}(\mathbf{P_j})}{\lambda_{max}(\mathbf{P_j})}\right). \tag{17}$$

So K_j and τ_j are inversely related. In fact,

$$K_j = \frac{\tau_j}{\tau_j + \lambda_j \ln\left(\frac{\lambda_{min}(\mathbf{P_j})}{\lambda_{max}(\mathbf{P_j})}\right)} \tag{18}$$

by (8) and (16). Thus, as K_j increases, τ_j decreases, and even though more time might be wasted relative to τ_j, this dwell time may be small enough that the wasted time is insignificant. On the other hand, as τ_j increases, K_j decreases even for ill-conditioned systems, implying that even though dwell time may be unavoidably long, little time will be wasted relative to this. This tempers the severity of the issue engendered by ill-conditioned systems.

4.4. DISSCUSSION AND COMPARISON

An evaluation of the strengths and weaknesses of the proposed method is now presented, along with a comparison to the existing approach of (16).

To begin, there are several underlying assumptions required for the success of the proposed method:

1. It is assumed that the linear model of the nonlinear switched system is “close enough," so that each ball B_j is contained in the locally stable region of the nonlinear mode j.

2. The dwell times were developed with the worst-case convergence rates of the Lyapunov functions for the linear system approximations, so it is assumed that the decay rates of these functions effectively approximate actual state convergence rates in the true nonlinear system.

In practice, engineers can attempt to analyze whether states in B_j will converge to $\mathbf{X_j}$ to generate confidence in the validity of the first assumption. Also, for many realistic and highly complex nonlinear systems, these assumptions are essentially necessary, as direct nonlinear stability proofs are nearly unattainable. The assumptions make obtaining dwell times practical.

This implementation advantage is highlighted by analysis of (16), which develops a method for procuring dwell times that does not rely on these assumptions but has similar structure to what has been proposed here. While it is failsafe, it is not always practical for high order systems.

The method of (16) constructs a connected set $\mathcal{L}$ which is the union of Lyapunov level sets over all subsystems, just like $\cup_J H_j$ in this paper. It then calculates a universal minimum dwell time σ which guarantees that the states will remain in $\mathcal{L}$ after finite time, regardless of the initial location of states. While this is an advantage, it requires assuming that each subsystem is globally exponentially stable. This is a luxury that is rarely present in real world systems. To obtain σ, (16) creates a set $\mathcal{N}$ that is analogous to $\cup_J b_j$ in this paper. There are then two intermediate quantities that must be determined:

$$\xi_j = \max_{\mathbf{x}\in\mathcal{N}} V_j(\mathbf{x}) \tag{19}$$

$$\mu = \max_{\mathbf{x}\notin\mathcal{N}} \frac{V_i(\mathbf{x})}{V_j(\mathbf{x})}; i, j \in J \tag{20}$$

The former term is analogous to C_j, because $V_j(\mathbf{x}) < C_j$ for all $\mathbf{x} \in \cup_J b_j$. The latter is used to ensure that any initial state values will converge to $\mathcal{L}$ under σ. In the absence of analytical insight, computing (19) requires solving N many constrained optimization problems, and computing (20) requires $N(N-1)$ many more for a system with N modes. By contrast, the presented approach requires solving only one such problem to select ball sizes. The computational advantage is clear, especially in higher order systems with numerous modes. Once all quantities have been calculated in (16), σ is found as

$$\sigma = \frac{\log(\mu)}{\epsilon}, \tag{21}$$

where ϵ is a positive number such that $\dot{V}_j \leq -\epsilon V_j$ for all j. It can be considered that

$$\frac{1}{\epsilon} = \max_{j \in J} \lambda_j \tag{22}$$

since λ_j is the smallest value such that $\dot{V}_j \leq -\frac{V_j}{\lambda_j}$. Therefore, $\sigma \geq \tau_j$ for all j, unless μ compensates for the conservatism introduced by ϵ.

As one final point of analysis, because the convergence rate in (4) was selected in a worst-case manner, it can sometimes be too conservative to be practical for minimum dwell times. In reality, the system states and Lyapunov functions sometimes converge much faster than this upper bound. When this occurs, an alternative method that obtains shorter dwell times may be necessary. Such a method is presented in the next section. It relies on one further assumption, which weakens its mathematical certainty, but this sacrifice may be required for practicality.

5. DWELL TIMES FROM SETTLING TIMES

If the rate of convergence in (4) is impractically conservative for a particular system, more practical dwell times can be obtained by a slight alteration of the outlined approach. Instead of computing dwell times from the worst-case Lyapunov convergence rates, they can be procured from the system settling time approximations. For a linearized mode of the form (7), this approximation is given by

$$t_s = \frac{\log(\rho)}{|\zeta_j|}, \tag{23}$$

where ζ_j is the real part of the dominant eigenvalue of $\mathbf{A_j}$, and ρ is the settling percent. This approximates the time that is required for $\|\tilde{\mathbf{x}}_j\|$ to converge such that $\|\tilde{\mathbf{x}}_j(t_0+t_s)\| \leq \rho\|\tilde{\mathbf{x}}_j(t_0)\|$, where $\tilde{\mathbf{x}}_j(t_0)$ is an initial state location.

With this in mind, B_j and b_j for each mode can be determined almost exactly as before, except that each weight α_j can be chosen as $\frac{1}{|\zeta_j|}$, because dwell times will be found from settling times which are made larger as $\frac{1}{|\zeta_j|}$ increases. Then, assuming the system states are within B_j upon switching to mode j, the worst-case initial value of $\|\tilde{\mathbf{x}}_j\|$ is R_j. Thus, $\rho_j = \frac{r_j}{R_j}$ ensures that the time given by (23) can be used as a minimum dwell time for $\|\tilde{\mathbf{x}}_j\|$ to converge within r_j of $\mathbf{X}_j$. From this the result of Theorem 3.1 can be proven just as before. So, alternative dwell times can be computed as

$$\tau_j = \frac{\log\left(\frac{r_j}{R_j}\right)}{|\zeta_j|}. \tag{24}$$

This approach may dramatically reduce dwell times, but its disadvantage is that an additional approximation is necessary, granting less mathematical certainty that the system will always be stable under the resulting dwell times. However, if the settling time

approximation is close enough, then the results of Theorem 3.1 can still be expected to hold. To maximize confidence, it is best to use equation (8) as much as practical, and then to use (24) for any remaining modes.

6. SIMULATIONS

6.1. BOOST CONVERTER

A MATLAB script was created to simulate the proposed methods for various switched systems. As an initial example, consider a boost converter as a switched system, where switching takes place in the load. The equivalent circuit is pictured in Figure 5.

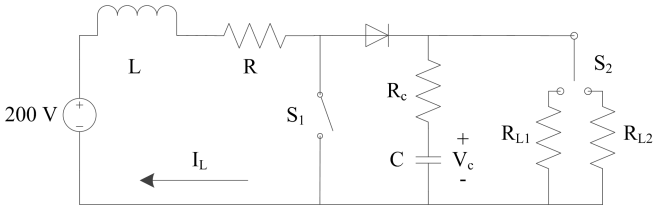

Figure 5. Boost converter circuit

The state-space model for this system can be derived as

$$\begin{pmatrix} \dot{I}_L \\ \dot{V}_C \end{pmatrix} = \begin{pmatrix} -\left(\frac{R_c R+u(DR_c+R)}{L(u+R_c)}\right) I_L - \left(\frac{Du}{L(u+R_c)}\right) V_C \\ \\ \left(\frac{Du}{C(u+R_c)}\right) I_L - \left(\frac{1}{C(u+R_c)}\right) V_C \end{pmatrix}, \tag{25}$$

where D is the duty cycle and u is the input that is discretely switched between R_{L1} and R_{L2}. In this simulation, system parameters are chosen as $D = 0.5$, $R = R_c = 0.01\Omega$, $C = 0.12$mF, $L = 0.95$mH, $R_{L1} = 30\Omega$, and $R_{L2} = 500\Omega$. If $u = R_{L1}$ corresponds to mode 1 and $u = R_{L2}$ corresponds to mode 2, the equilibrium points are computed as

$$\mathbf{X_1} = \begin{pmatrix} 21.6223 \text{ A} \\ 399.3345 \text{ V} \end{pmatrix}; \mathbf{X_2} = \begin{pmatrix} 1.5998 \text{ A} \\ 399.9600 \text{ V} \end{pmatrix},$$

and the ball sizes and minimum dwell times by Lyapunov convergence rates are

$$\begin{pmatrix} R_1 \\ r_1 \\ R_2 \\ r_2 \end{pmatrix} = \begin{pmatrix} 26.8845 \\ 0.6173 \\ 25.6476 \\ 1.8542 \end{pmatrix}; \begin{pmatrix} \tau_1 \\ \tau_2 \end{pmatrix} = \begin{pmatrix} 0.1465 \text{ s} \\ 1.0058 \text{ s} \end{pmatrix}.$$

Figure 6 shows the behavior of the system over 10 seconds if it is switched as quickly as possible (as soon as each minimum dwell time passes). The black circles depicted are b_1 and b_2. In addition to overall system stability, it can be seen that the system states are in their appropriate ball whenever the system switches.

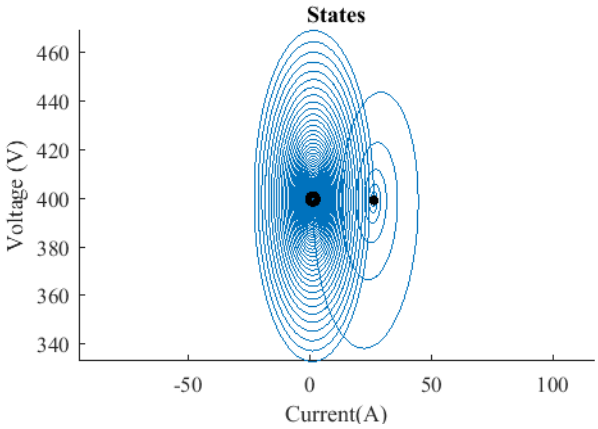

Figure 6. Switched boost converter under minimum dwell times

While the system is stable under its minimum dwell times, it is certainly not so for all switched signals. Figure 7 shows system behavior under the state-dependent "worst-case" switching of section 2.2. Though it is somewhat difficult to tell, the voltage in Figure 7 becomes as low as $V_c = -8.0006V$. In an actual boost converter, this negative voltage

would destroy the converter, effectively rendering such behavior unstable. The largest time delay between any two switching actions causing this instability was 0.0021s, which greatly violates the minimum dwell times found for the system.

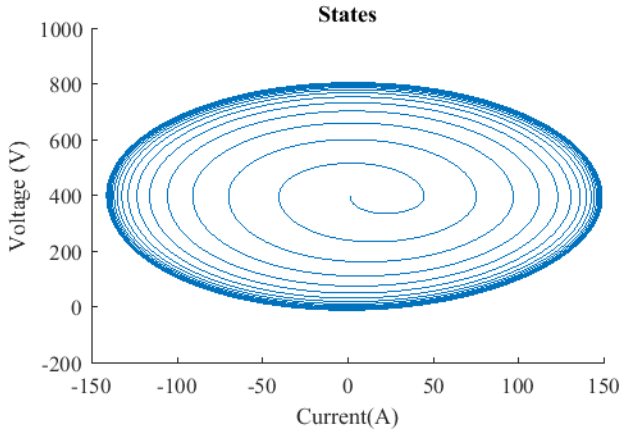

Figure 7. Unstable behavior without minimum dwell times

To demonstrate the effective application of Remark (1), consider the introduction of a third mode, with $R_{L1} = 10\Omega$, $R_{L2} = 100\Omega$, and $R_{L3} = 1000\Omega$. Direct implementation of the stability result yields

$$\begin{pmatrix} R_1 \\ r_1 \\ R_2 \\ r_2 \\ R_3 \\ r_3 \end{pmatrix} = \begin{pmatrix} 82.6838 \\ 0.4671 \\ 72.0956 \\ 11.0553 \\ 79.2939 \\ 3.8570 \end{pmatrix}; \begin{pmatrix} \tau_1 \\ \tau_2 \\ \tau_3 \end{pmatrix} = \begin{pmatrix} 0.0674\ \text{s} \\ 1.4998\ \text{s} \\ 0.2617\ \text{s} \end{pmatrix}$$

.

However, if it is imposed that R_{L1} cannot switch directly to R_{L3} and vice versa, conditions can be relaxed according to Remark (1) to yield

$$\begin{pmatrix} R_1 \\ r_1 \\ R_2 \\ r_2 \\ R_3 \\ r_3 \end{pmatrix} = \begin{pmatrix} 72.9002 \\ 0.6175 \\ 72.2459 \\ 1.2718 \\ 8.4701 \\ 8.4701 \end{pmatrix}; \begin{pmatrix} \tau_1 \\ \tau_2 \\ \tau_3 \end{pmatrix} = \begin{pmatrix} 0.0631 \text{ s} \\ 0.4564 \text{ s} \\ 0.3824 \text{ s} \end{pmatrix}$$

.

The average of the dwell times in the first case was 0.6097s compared to 0.3006s in the second. Also, the average large ball size was 78.0244 in the first case compared to 51.2054 in the second. This is a 50.7% decrease in the average of the dwell times and a 34.37% reduction in average large ball size, so Remark (1) grants considerable gains in this system.

6.2. MICROGRID

As a more complex but practical example, consider the two-inverter microgrid system from (25). This system has 35 states, and switching is governed by the load on the microgrid. All parameter values used in this simulation are the same as in (25). The load consists of two parallel impedances, one of which is held constant at 25 Ω and 7.5 mH while the other switches between the following inputs:

$$\begin{pmatrix} u_1 \\ u_2 \\ u_3 \end{pmatrix} = \begin{pmatrix} 25\ \Omega, 15\ \text{mH} \\ 12.5\ \Omega, 5.6\ \text{mH} \\ 50\ \Omega, 25\ \text{mH} \end{pmatrix}. \tag{26}$$

Computing the dwell times by (8) produces

$$\begin{pmatrix} \tau_1 \\ \tau_2 \\ \tau_3 \end{pmatrix} = \begin{pmatrix} 2.6054 \times 10^8 \text{ s} \\ 2.6293 \times 10^8 \text{ s} \\ 2.5981 \times 10^8 \text{ s} \end{pmatrix}, \tag{27}$$

and these are completely impractical. Therefore, the dwell times are alternatively calculated by (24), resulting in

$$\begin{pmatrix} R_1 \\ r_1 \\ R_2 \\ r_2 \\ R_3 \\ r_3 \end{pmatrix} = \begin{pmatrix} 317.7769 \\ 168.3885 \\ 471.4169 \\ 9.7486 \\ 467.6587 \\ 13.5068 \end{pmatrix}; \begin{pmatrix} \tau_1 \\ \tau_2 \\ \tau_3 \end{pmatrix} = \begin{pmatrix} 0.2701 \text{ s} \\ 1.5892 \text{ s} \\ 1.4342 \text{ s} \end{pmatrix}.$$

These dwell times are easily implementable. A simulation was run that switches to a randomly selected destination mode immediately once the current minimum dwell time passes. The state norms are shown in Figure 4. Each switching instance is marked by a dotted vertical line, while the dotted horizontal lines represent the thresholds r_j that $\|\tilde{\mathbf{x}}_j\|$ must reach before the next switching instance. The figure shows that $\|\tilde{\mathbf{x}}_j\|$ reaches this goal each time, and the system is thus stable for the duration of the simulation.

6.3. POWER GRID

This example will apply the settling time method to a larger scale grid model. Consider a power system with seven buses connected to an isochronous generator, droop generator, and five microgrids (SST's). All nodes are interconnected by lines with impedances as shown in Figure 9. Each bus is also connected to a load, and a change in any of the loads constitutes a system switching event.

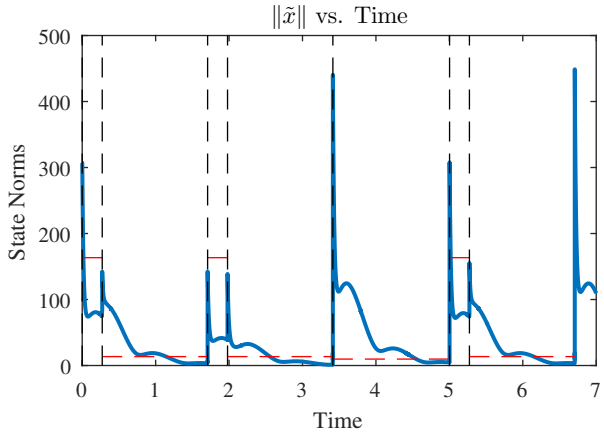

Figure 8. Microgrid under minimum dwell times

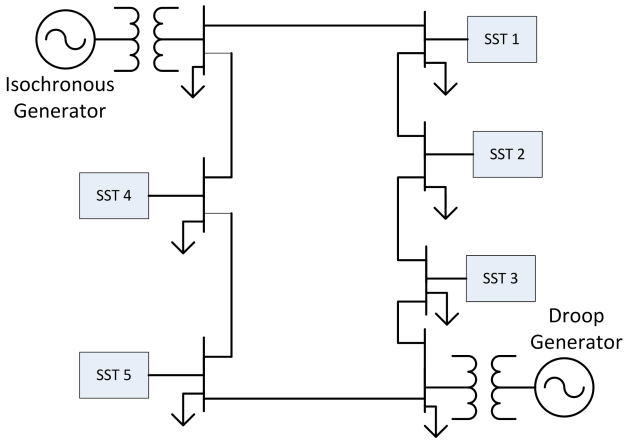

Figure 9. Seven node power grid

The five SST's are each modeled by the equations in (25), and the isochronous and droop generator equations were developed from models in (23) and (24). These together with Kirchhoff equations for the loads and lines total 115 equations that comprise the state space system model.

In this simulation, each load was given a default value of 10 Ω and 1.5 mH. Three buses could switch to different loads: the load on bus SST 1 could switch to 20 Ω and 0.75 mH, bus SST 2 could switch to 100 Ω and 1.5 mH, and the droop generator bus could switch to 50 Ω and 2.5 mH. All eight resulting combinations were considered as valid switching configurations.

In practice, two loads could not switch at the same time, so a switch could not occur between modes with more than one load discrepancy. Therefore, Remark (1) can be applied to relax the requirements on ball sizes. This example was run with and without this constraint relaxation. In the first case, large ball sizes and dwell times were found as

$$\begin{pmatrix} R_1 \\ R_2 \\ R_3 \\ R_4 \\ R_5 \\ R_6 \\ R_7 \\ R_8 \end{pmatrix} = \begin{pmatrix} 212.9615 \\ 176.2163 \\ 212.8434 \\ 179.574 \\ 176.1039 \\ 211.1805 \\ 179.6849 \\ 211.3002 \end{pmatrix}; \begin{pmatrix} \tau_1 \\ \tau_2 \\ \tau_3 \\ \tau_4 \\ \tau_5 \\ \tau_6 \\ \tau_7 \\ \tau_8 \end{pmatrix} = \begin{pmatrix} 8.6924 \text{ s} \\ 4.2189 \text{ s} \\ 8.6902 \text{ s} \\ 4.7178 \text{ s} \\ 4.2177 \text{ s} \\ 8.4272 \text{ s} \\ 4.7184 \text{ s} \\ 8.4298 \text{ s} \end{pmatrix}.$$

After relaxing restrictions, these became

$$\begin{pmatrix} R_1 \\ R_2 \\ R_3 \\ R_4 \\ R_5 \\ R_6 \\ R_7 \\ R_8 \end{pmatrix} = \begin{pmatrix} 211.4528 \\ 174.7076 \\ 210.8302 \\ 191.1791 \\ 174.0907 \\ 201.1402 \\ 172.3609 \\ 197.0794 \end{pmatrix}; \begin{pmatrix} \tau_1 \\ \tau_2 \\ \tau_3 \\ \tau_4 \\ \tau_5 \\ \tau_6 \\ \tau_7 \\ \tau_8 \end{pmatrix} = \begin{pmatrix} 6.9756 \text{ s} \\ 4.7876 \text{ s} \\ 9.7885 \text{ s} \\ 5.525 \text{ s} \\ 4.0645 \text{ s} \\ 8.1642 \text{ s} \\ 4.4379 \text{ s} \\ 7.9006 \text{ s} \end{pmatrix}.$$

The average of the dwell times in the first case is 6.51s compared to 6.4555s in the second, and the average of the first large ball sizes was 194.9831 compared to 191.6051 in the second case. Both averages dropped only slightly due to the relaxed conditions. The amount of benefit achieved by Remark (1) is entirely dependent on the particular system and modes, as shown between this example and example 6.1.

7. CONCLUSION

This paper developed a practical method for ensuring the stability of switched systems with multiple equilibria using modal dwell times from Lyapunov functions. Efficacy was demonstrated with examples drawn from power systems and electronics. The limitations of this method include conservatism in the Lyapunov function method, and some uncertainty due to approximation in the settling time technique. However, both possess the advantage of simple applicability and ease of algorithmic implementation. This was designed so that the method would be attractive and helpful to practicing control engineers. To further applicability, future work could extend this method to the case in which the set of possible subsystems is not countable, but instead restricted by some variable parameter. This extension might provide a better model for real world systems in which all potential modes aren't exactly known, but the general range of equilibria is.

ACKNOWLEDGEMENTS

Work supported by National Science Foundation Award 1505610.

REFERENCES

[1] D. Liberzon, *Switching in Systems and Control*. New York, NY: Birkhäuser, 2003.

[2] J. P. Hespanha and A. S. Morse, "Stability of switched systems with average dwell time," in *38th Conference on Decision and Control*, 1999.

[3] D. Liberzon and A. S. Morse, "Basic problems in stability and design of switched systems," *IEEE Control Systems Magazine*, vol. 19, October 1999.

[4] X. Gao, D. Liberzon, J. Liu, and T. Basar, "Unified stability criteria for slowly time-varying and switched linear systems," *Automatica*, 2018.

[5] X. Zhao, L. Zhang, P. Shi, and M. Liu, "Stability and stabilization of switched linear systems with mode-dependent average dwell time," *IEEE Transactions on Automatic Control*, vol. 57, pp. 1809–1815, July 2012.

[6] X. Zhao, S. Yin, H. Li, and B. Niu, "Switching stabilization for a class of slowly switched systems," *IEEE Transactions on Automatic Control*, vol. 60, pp. 221–226, 2015.

[7] M. S. Branicky, "Multiple lyapunov functions and other analysis tools for switched and hybrid systems," *IEEE Transactions on Automatic Control*, vol. 43, pp. 475–482, April 1998.

[8] J. C. Geromel and P. Colaneri, "Stability and stabilization of continuous-time switched linear systems," *IEEE Control Systems Magazine*, vol. 45, no. 5, pp. 1915–1930, 2006.

[9] A. Kundu and D. Chatterjee, "Stabilizing switching signals for switched systems," *IEEE Transactions on Automatic Control*, vol. 60, pp. 882–888, March 2015.

[10] J. Lee and G. E. Dullerud, "Uniformly stabilizing sets of switching sequences for switched linear systems," *IEEE Transactions on Automatic Control*, vol. 52, pp. 868–874, May 2007.

[11] R. A. Decarlo, M. S. Branicky, S. Pettersson, and B. Lennartson, "Perspectives and results on the stability and stabilizability of hybrid systems," *Proceedings of the IEEE*, vol. 88, no. 7, pp. 1069–1082, July 2000.

[12] G. Davrazos and N. T. Koussoulas, "A review of stability results for switched and hybrid systems," in *Proc. 9th Mediterranean Conference on Control and Automation*, 2001.

[13] H. Lin and P. J. Antsaklis, "Stability and stabilizability of switched linear systems: A survey of recent results," *IEEE Transactions on Automatic Control*, vol. 54, pp. 308–322, February 2009.

[14] X. Xu and G. Zhai, "Practical stability and stabilization of hybrid and switched systems," *IEEE Transactions on Automatic Control*, vol. 50, no. 11, pp. 1897–1903, Nov 2005.

[15] G. Zhai and A. N. Michel, "Generalized practical stability analysis of discontinuous dynamical systems," in *42nd IEEE International Conference on Decision and Control (IEEE Cat. No.03CH37475)*, vol. 2, Dec 2003, pp. 1663–1668 Vol.2.

[16] T. Alpcan and T. Basar, "A stability result for switched systems with multiple equilibria," *Dynamics of Continuous, Discrete, and Impulsive Systems*, vol. 17, pp. 949–958, May 2010.

[17] F. Blanchini, D. Casagrande, and S. Miani, "Modal and transition dwell time computation in switching systems: A set-theoretic approach," *Automatica*, vol. 46, pp. 1477–1482, July 2010.

[18] R. Kuiava, R. A. Ramos, H. R. Pota, and L. F. C. Alberto, "Practical stability of continuous-time switched systems without a common equilibria and governed by a time-dependent switching signal," in *2011 9th IEEE International Conference on Control and Automation (ICCA)*, Dec 2011, pp. 1156–1161.

[19] R. Kuiava, R. A. Ramos, L. F. C. Alberto, and H. R. Pota, "Practical stability assessement of distributed synchronous generators under load variations," in *2013 IEEE International Symposium on Circuits and Systems (ISCAS2013)*, May 2013, pp. 457–460.

[20] G. Chesi, P. Colaneri, J. C. Geromel, and R. Middleton, "Computing upper-bounds of the minimum dwell time of linear switched systems via homogeneous polynomial lyapunov functions," in *American Control Conference Proc.*, 2010, pp. 2487–2492.

[21] H. K. Khalil, *Nonlinear Systems*. Upper Saddle River, NJ: Prentice Hall, 2001.

[22] M. Caramia and P. Dell'Olmo, *Multi-objective Management in Freight Logistics*. London, UK: Springer-Verlag, 2008.

[23] R. Krishnan, *Electric Motor Drives: Modeling, Analysis, and Control*. Upper Saddle River, NJ: Prentice Hall, 2001.

[24] P. C. Krause, O. Wasynczuk, and S. D. Sudhoff, *Analysis of Electric Machinery and Drive Systems*, 2nd ed. Piscataway, NJ: IEEE Press, 2002.

[25] M. Rasheduzzaman, J. A. Mueller, and J. W. Kimball, "An accurate small-signal model of inverter-dominated islanded microgrids using dq reference frame," *IEEE Journal of Emerging and Selected Topics in Power Electronics*, vol. 2, December 2014.

[26] Z. Gajić and M. T. J. Qureshi, *Lyapunov Matrix Equation in System Stability and Control*. San Diego, CA: Academic Press, 1995.

[27] H. G. Kwatny and G. L. Blankenship, *Nonlinear Control and Analytical Mechanics*. New York, NY: Birkhäuser, 2000.

SECTION

3. SUMMARY AND CONCLUSIONS

This thesis develops and demonstrates a practical method for certifying the stability of switched systems with multiple operating points. The approach utilizes Lyapunov function convergence rates of linearized subsystems to procure dwell times and restrict admissible switching signals. The design is practical and straightforward, and is intended for use in power system stability and security. Some assumptions were made to weaken conservatism, such as linearization and the use of settling time approximations. However, these concessions are often critical in complex real-world applications, as the full nonlinear analysis of an intricate Smart Grid is a formidable task.

Two compelling areas for future work exist, and both are in progress. First, a model for switching a microgrid between islanded and grid-tied configurations should be created and analyzed with the proposed method. This thesis primarily considered load variations as switching actions, but microgrid switching motivated much of this study and should be examined in detail. Second, in many practical cases prior knowledge about the precise system modes may not exist. For example, in the case of load switches on the power grid, an engineer may not know exactly which values the load might take. Instead, the general range of expected load values might be available. In such cases it is more accurate to view the switched system as having an uncountable set of possible subsystems that are limited by some bounded parameter. Since uncountable dwell times cannot be generated, the proposed method should be tailored to this case.

Some work has been completed in this regard, which may be detailed in the future. For a general description, the proposed adaptation is as follows. First, Latin Hypercube sampling can be used to sample the resulting equilibria from a representative range of the

bounded input parameters (such as the loads on a power grid). The geometric center of these operating points can be found, and a large ball can be chosen that contains all samples. Several calculations must be made online. Upon a switching action, the new operating point must be computed. Also, the largest ball that is contained in the first ball and centered on the new operating point must be found. Using the initial location of states upon switching, a settling time can be calculated that ensures the states are within this ball and thus are within the large ball after the dwell time has passed. This structure will ensure that states are always in this large ball upon switching actions.

Work has been done to test this idea. A MATLAB script was created to execute this algorithm on the boost converter model. Here, the load could take any value from 10 Ω to 100 Ω. The system was switched to a new random subsystem as soon as the calculated dwell time passed. The output is displayed in Figure 3.1.

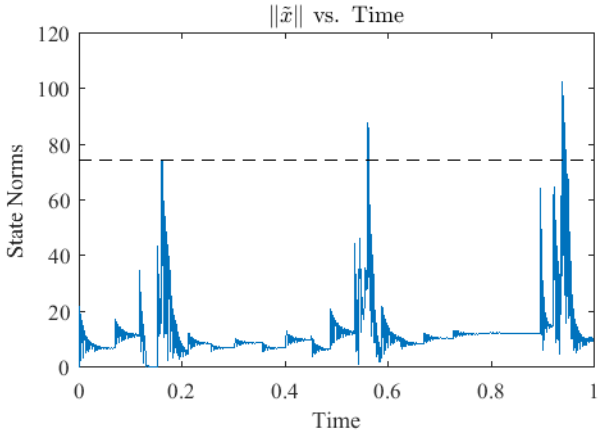

Figure 3.1. Boost converter switching with unknown modes

The black dashed line is the radius of the large ball, and the y-axis depicts the norm of the states from the center of the ball. The oscillations encountered upon switching reveal the spiraling of states about new equilibrium points, which appears as oscillations from the perspective of the geometric center. Note that the states are within the large ball upon every

switching action. This will bound the states to the union of the largest possible Lyapunov level sets within the ball over all modes. While this shows promise, work remains to be done to formalize the process and produce cleaner simulations.

Ultimately, this thesis presented an algorithm intended to protect switched systems against instability caused by switching, especially for systems that are susceptible to such attacks like the Smart Grid. While work is left to be done, the author hopes that the ideas in this thesis will be applied towards the stability and security of switched systems in their many contexts.

APPENDIX

MATLAB SCRIPT

This Appendix contains the MATLAB code written to perform the algorithms detailed in this thesis.

Main. This code serves to synthesize all subprocesses.

```
%Main
clc
clearvars
%%
% The only inputs are all the system dynamics from fxu.m,
% and the input matrix,
% U, which defines the system modes. The U matrix should
% have an input going down a column, with the number
% of columns corresponding to the discrete number of
% inputs (and thus modes).

dim = 2; %Dimension of system
U = [30,500]; %Boost Converter
[A,gam,modes] = resgamv2(U,dim);

% Columns of 'modes' are operating points,
% number of rows is the dimension. A is an array where A{i}
% is the linearization matrix of the ith mode.
```

```
%%
%Get the number of modes
m = length(modes(1,:));

%%
% This section sets up the path matrix, Mark. That is, this
% matrix shows whether or not a path exists from mode x to
% mode y. If there is no path from x to y, then the big
% ball of x mustn't contain the small of y, and so we can
% use that info to tailor our constraints to the problem.
% Mark(1,3) = 0 implies that there is no path from mode 1.
% to mode 3.

Mark = ones([m,m]);

%%
% We now need to obtain the P matrices of the Lyapunov
% function, as well as the min and max eigenvalues for
% each P matrix. We obtain these and put all of the
% information in arrays. We also define our alpha weights
% (to be used later) from the time constants from the
% Lyapunov matrices P and Q.

    eigmax = zeros(1,m);
    eigmin = zeros(1,m);
    tc = zeros(1,m);
```

```
for i = 1:m
    [eigmax(i),eigmin(i),tc(i)] = resweights(A{i});
end

%%
% The function below uses all of the information found so
% far to determine the optimal sizes of the balls for each
% mode. It needs to know the operating points, alpha and
% gamma weights, and the path matrix.

    [radii] = resballs(modes,tc,gam,Mark);

%%
% Now we take all of the radii of the balls along with the
% eigenvalues obtained before to translate back to the
% sizes of the lyapunov level sets. From here one can
% check the validity of the ball sizes.

    [biglevs,littlelevs,K] =
    ...reslevsets(radii,eigmin,eigmax,m);

% Finally, the dwell times are calculated in the
% function below.

    [waittimes] = restimes(biglevs,littlelevs,tc,m);
    modes
    waittimes
```

```
% end
```

Dynamics. This function contains all the dynamics of the switched system. The islanded microgrid model is shown here as an example.

```
function f = fxu(x,u)
%%
% Microgrid extended model, 2 inverters, islanded.

% Constant values
kpd = 0.5;
kpq = 0.5;
kid = 25;
kiq = 25;
kpcd = 1;
kpcq = 1;
kicd = 100;
kicq = 100;
kpPLL = 0.25;
kiPLL = 2;
Lf = 0.0042;
Lc = 0.0005;
Cf = 0.000015;
omegac = 50.26;
omegacPLL = 7853.98;
m = 0.001;
rn = 1000;
rline = 0.15;
```

```
rf = 0.5;
rc = .09;
Rd = 2.025;
omegan = 377;
n = .001;
VOQN = 85;
Lline = .0004;

% State assignment
P1 = x(1);
Q1 = x(2);
vodf1 = x(3);
phiPLL1 = x(4);
phid1 = x(5);
phiq1 = x(6);
gamd1 = x(7);
gamq1 = x(8);
ild1 = x(9);
ilq1 = x(10);
iod1 = x(11);
ioq1 = x(12);
vod1 = x(13);
voq1 = x(14);
P2 = x(15);
Q2 = x(16);
vodf2 = x(17);
phiPLL2 = x(18);
```

```
phid2 = x(19);
phiq2 = x(20);
gamd2 = x(21);
gamq2 = x(22);
ild2 = x(23);
ilq2 = x(24);
iod2 = x(25);
ioq2 = x(26);
vod2 = x(27);
voq2 = x(28);
iloadd1 = x(29);
iloadq1 = x(30);
iloadd2 = x(31);
iloadq2 = x(32);
ilined = x(33);
ilineq = x(34);
delt2 = x(35);

% Input assignment
Rload1 = u(1);
Lload1 = u(2);
Rload2 = u(3);
Lload2 = u(4);

% Intermediate variables
vbD1 = rn*(iod1 - ilined - iloadd1);
vbQ1 = rn*(ioq1 - ilineq - iloadq1);
```

```
vbD2 = rn*((iod2*cos(delt2)+ioq2*sin(delt2)) + ilined
... - iloadd2);
vbQ2 = rn*((ioq2*cos(delt2)-iod2*sin(delt2)) + ilineq
... - iloadq2);
vbd1 = vbD1;
vbq1 = vbQ1;
vbd2 = vbD2*cos(delt2) - vbQ2*sin(delt2);
vbq2 = vbD2*sin(delt2) + vbQ2*cos(delt2);

% Dynamics
f(1) = -P1*omegac + 1.5*omegac*(vod1*iod1 + voq1*ioq1);
f(2) = -Q1*omegac + 1.5*omegac*(voq1*iod1 - vod1*ioq1);
f(3) = omegacPLL*vod1 - omegacPLL*vodf1;
f(4) = -vodf1;
f(5) = 377 - kpPLL*vodf1 + kiPLL*phiPLL1 - omegan + m*P1;
f(6) = VOQN - n*Q1 - voq1;
f(7) = kid*phid1 + kpd*(377 - kpPLL*vodf1...
    + kiPLL*phiPLL1 - omegan + m*P1)- ild1;
f(8) = kiq*phiq1 + kpq*(VOQN - n*Q1 - voq1) - ilq1;
f(9) = (1/Lf)*(-rf*ild1 - omegan*Lf*ilq1 + kicd*gamd1 + ...
    kpcd*(kid*phid1 + kpd*(377 - kpPLL*vodf1 +...
    kiPLL*phiPLL1 - omegan + m*P1)- ild1)...
    - vod1) + (377 - kpPLL*vodf1 + ...
    kiPLL*phiPLL1)*ilq1;
f(10) = (1/Lf)*(-rf*ilq1 + omegan*Lf*ild1 + kicq*gamq1 + ...
    kpcq*(kiq*phiq1 + kpq*(VOQN - n*Q1 - voq1) - ilq1) - ...
    voq1) - (377 - kpPLL*vodf1 + kiPLL*phiPLL1)*ild1;
```

```
f(11) = (1/Lc)*(-rc*iod1 + vod1 - vbd1) + (377...
 - kpPLL*vodf1 + kiPLL*phiPLL1)*ioq1;
f(12) = (1/Lc)*(-rc*ioq1 + voq1 - vbq1) -...
(377 - kpPLL*vodf1 + kiPLL*phiPLL1)*iod1;
f(13) = (1/Cf)*(ild1 - iod1) + (377 - kpPLL*vodf1 + ...
    kiPLL*phiPLL1)*voq1 + Rd*(((1/Lf)*(-rf*ild1 - ...
    omegan*Lf*ilq1 + kicd*gamd1 + kpcd*(kid*phid1 + ...
    kpd*(377 - kpPLL*vodf1 + ...
    kiPLL*phiPLL1 - omegan + m*P1)- ...
    ild1) - vod1) + (377 - kpPLL*vodf1...
    + kiPLL*phiPLL1)*ilq1 )...
    - ((1/Lc)*(-rc*iod1 + vod1...
    - vbd1) + (377 - kpPLL*vodf1 + ...
    kiPLL*phiPLL1)*ioq1 ));
f(14) = (1/Cf)*(ilq1 - ioq1 )...
- (377 - kpPLL*vodf1 + ...
    kiPLL*phiPLL1)*vod1...
    + Rd*(((1/Lf)*(-rf*ilq1 + ...
    omegan*Lf*ild1 + kicq*gamq1...
    + kpcq*(kiq*phiq1 + ...
    kpq*(VOQN - n*Q1 - voq1)...
    - ilq1) - voq1) + (377 - ...
    kpPLL*vodf1 + kiPLL*phiPLL1)*ild1 )...
     -((1/Lc)*(-rc*ioq1 + ...
    voq1 - vbq1) - ...
    (377 - kpPLL*vodf1 + kiPLL*phiPLL1)*iod1 ));
f(15) = -P2*omegac + 1.5*omegac*(vod2*iod2 + voq2*ioq2 );
```

```
f(16) = -Q2*omegac + 1.5*omegac*(voq2*iod2 - vod2*ioq2);
f(17) = omegacPLL*vod2 - omegacPLL*vodf2;
f(18) = -vodf2;
f(19) = 377 - kpPLL*vodf2 + ...
    kiPLL*phiPLL2 - omegan + m*P2;
f(20) = VOQN - n*Q2 - voq2;
f(21) = kid*phid2 + ...
    kpd*(377 - kpPLL*vodf2 + kiPLL*phiPLL2 - ...
    omegan + m*P2)- ild2;
f(22) = kiq*phiq2 + kpq*(VOQN - n*Q2 - voq2) - ilq2;
f(23) = (1/Lf)*(-rf*ild2 - ...
    omegan*Lf*ilq2 + kicd*gamd2 + ...
    kpcd*(kid*phid2 + ...
    kpd*(377 - kpPLL*vodf2 + kiPLL*phiPLL2 - ...
    omegan + m*P2)- ild2) - vod2) + (377 - kpPLL*vodf2 + ...
    kiPLL*phiPLL2)*ilq2;
f(24) = (1/Lf)*(-rf*ilq2 + omegan*Lf*ild2 + kicq*gamq2 + ...
    kpcq*(kiq*phiq2 + kpq*(VOQN - n*Q2 - voq2) - ilq2) - ...
    voq2) - (377 - kpPLL*vodf2 + kiPLL*phiPLL2)*ild2;
f(25) = (1/Lc)*(-rc*iod2 + vod2 - vbd2) + (377 - ...
    kpPLL*vodf2 + kiPLL*phiPLL2)*ioq2;
f(26) = (1/Lc)*(-rc*ioq2 + voq2 - vbq2) - (377 - ...
    kpPLL*vodf2 + kiPLL*phiPLL2)*iod2;
f(27) = (1/Cf)*(ild2 - iod2) + (377 - kpPLL*vodf2 + ...
    kiPLL*phiPLL2)*voq2 + Rd*(((1/Lf)*(-rf*ild2 - ...
    omegan*Lf*ilq2 + kicd*gamd2 + kpcd*(kid*phid2 + ...
    kpd*(377 - kpPLL*vodf2 + kiPLL*phiPLL2 - omegan + ...
```

```
    m*P2)- ild2) - vod2) + (377 - kpPLL*vodf2 + ...
    kiPLL*phiPLL2)*ilq2) - ((1/Lc)*(-rc*iod2 + vod2 - ...
    vbd2) + (377 - kpPLL*vodf2 + kiPLL*phiPLL2)*ioq2));
f(28) = (1/Cf)*(ilq2 - ioq2) - (377 - kpPLL*vodf2 + ...
    kiPLL*phiPLL2)*vod2 + Rd*(((1/Lf)*(-rf*ilq2 + ...
    omegan*Lf*ild2 + kicq*gamq2 + kpcq*(kiq*phiq2 + ...
    kpq*(VOQN - n*Q2 - voq2) - ilq2) - voq2) + (377 - ...
    kpPLL*vodf2 + ...
    kiPLL*phiPLL2)*ild2)-((1/Lc)*(-rc*ioq2 +...
    voq2 - vbq2) - ...
    (377 - kpPLL*vodf2 + kiPLL*phiPLL2)*iod2));
f(29) = (1/Lload1)*(-Rload1*iloadd1 + vbD1) + (377 - ...
    kpPLL*vodf1 + kiPLL*phiPLL1)*iloadq1;
f(30) = (1/Lload1)*(-Rload1*iloadq1 + vbQ1) - (377 - ...
    kpPLL*vodf1 + kiPLL*phiPLL1)*iloadd1;
f(31) = (1/Lload2)*(-Rload2*iloadd2 + vbD2) + (377 - ...
    kpPLL*vodf2 + kiPLL*phiPLL2)*iloadq2;
f(32) = (1/Lload2)*(-Rload2*iloadq2 + vbQ2) - (377 - ...
    kpPLL*vodf2 + kiPLL*phiPLL2)*iloadd2;
f(33) = (1/Lline)*(-rline*ilined + vbD1 - vbD2) + ...
    (377 - kpPLL*vodf1 + kiPLL*phiPLL1)*ilineq;
f(34) = (1/Lline)*(-rline*ilineq + vbQ1 - vbQ2) - ...
    (377 - kpPLL*vodf1 + kiPLL*phiPLL1)*ilined;
f(35) = (377 - kpPLL*vodf1 + kiPLL*phiPLL1) - ...
    (377 - kpPLL*vodf2 + kiPLL*phiPLL2);
```

Operating Points and Linearizations. This function serves several purposes: it determines the stable operating point of each subsystem, obtains the linear approximation of each subsystem, and determines all γ weights.

```
function [A,rad,modes,maxeigs] = resgamv2(U,dim)
%%
% First we define the symbolic variables to be used.
Hu = sym('u',[1,length(U(:,1))]);
m = length(U(1,:));
X = sym('x',[1,dim]);

%%
% Here we find the stable operating points of
% the nonlinear system and put them into a matrix
% called 'modes.' We then find the Jacobian of the system,
% and from this obtain the A matrices for each mode,
% which give the linear approximations.
x0 = zeros([1,dim]);
modes = zeros([dim,m]);
for i = 1:m
    Ftemp = fxu(X,U(:,i));
    F = matlabFunction(Ftemp,'vars',{X});
    options =...
    optimset('MaxFunEvals',1000000,'MaxIter',1000000);
    oppoints = fsolve(F,x0,options);
    modes(:,i) = oppoints.';
end
```

```
J = jacobian(fxu(X,Hu),X);


A = cell(1,m);
maxeigs = zeros(m,1);
for i = 1:m
    A{i} = subs(J, [X,Hu], [(modes(:,i)).',U(:,i).']);
    A{i} = double(A{i});
    if max(real(eig(A{i}))) > 0
        error('The A matrix is not stable.')
    end
    maxeigs(i) = abs(max(real(eig(A{i}))));
end

%%
% Now we find our error term by taking the
% linearized system minus the actual system at U
% for each mode, and we normalize by dividing by the
% linearized system.
for i = 1:m
    E(:,i) = (A{i}*(X.' - modes(:,i)) - fxu(X,U(:,i)).');
    for j = 1:dim
        Co = coeffs(E(j,i));
        if max(Co) <= .00000001
            E(j,i) = 0;
        end
    end
end
```

```
%%
% Here we determine the "quality"
% of each linear approximation
% by a gradient ascent algorithm that determines how far
% from each operating point the approximation error equals
% or exceeds W. This will give the gamma weights.
rad = zeros([m,1]);
for i = 1:m
    N = norm(E(:,i));
    g = gradient(N,X);
    W = 0;
    iter = 0;
    point = modes(:,i);
        while W <= 20 && iter <= 20
            if g == 0
                W = 21;
                iter = 21;
                point = Inf([dim,1]);
            else
                G = subs(g,[X,Hu],...
                [point.' + 0.01,U(:,i).']);
                point = point + ((G)./norm(G));
                W = subs(N,[X,Hu],[point.',U(:,i).']);
                iter = iter + 1
            end
        end
```

```
    rad(i) = norm(modes(:,i) - point);
end
if rad == Inf(m,1)
    rad = zeros(m,1) + 1;
end

rad = 1./rad;

end
```

Lyapunov Solutions. This function solves the Lyapunov equation for each system mode and returns the smallest and largest eigenvalues of the solution for use later.

```
function [lammax,lammin,tc] = resweights(A)
%%
% All we do here is find the biggest and
% smallest eigenvalues of the P Lyapunov
% solution matrix. We also find our
% alpha weights based on the
% time constants yielded by P and Q.

Q = eye(length(A));

P = lyap(A,Q);
D = eig(Q);
E = eig(P);
lammax = max(E);
```

```
lammin = min(E);
lamminQ = min(D);
tc = lammax./lamminQ;
end
```

Ball Sizes. This script uses the MATLAB function fmincon to optimize the balls B_n and b_n for all n.

```
function [x] = resballs(P,a,g,Mark)

m = length(P(1,:));
n = length(P(:,1));

[row,col] = find(~Mark);

%%
% Create the inequality matrix to constrain
% the optimazation problem using
% the number of modes of the system.
A = zeros(m*(m-1)+m,2*m);
for i = 1:m
    v = zeros(m-1,2*m);
    v(:,(2*i)-1) = 1;
    w = [];
    for j = 1:m
        if(j == i)
        else
            w = [w, 2*j];
```

```
            end
        end
        for k = 1:m-1
            v(k,w(k)) = -1;
        end
        for l = 1:m-1

            A((l-1) + (i-1)*m - i + 2,:) = v(l,:);
        end
        A(m*(m-1)+ i,2*i-1) = 1;
        A(m*(m-1)+i,2*i) = -1;
    end
    A = A.*(-1);

%%
% Initialize a bottom left triangular
% matrix containing the distances from mode
% to mode based on the function input P,
% which is the matrix in which each column is
% the coordinates of one of the modes.

    X = zeros(m,m);
    for i = 1:m
        for j = 1:m
            if( i <= j)
                X(i,j) = 0;
            else
```

```
            X(i,j) = sqrt(sum((P(:,i)-P(:,j)).^2));
        end
    end
end
X = X.*(-1);

%%
% Using the matrix X defined above,
% create the vector of constant terms for
% the inequalities constraining the optimization problem.
B = zeros(m*(m-1)+ m,1);
for i = 1:m*(m-1)
    ytemp = find(A(i,:) == 1);
    y = (ytemp)/2;
    ztemp = find(A(i,:) == -1);
    z = (ztemp+1)/2;
    if(y>z)
        B(i,1) = X(y,z);
    else
        B(i,1) = X(z,y);
    end
end

%%
% Here is where we use the path information
% to eliminate the unnecessary constraints.
```

```
for i = 1:length(row)
    [c,~] = find(A([(col(i)-1)*m - col(i) + 2,...
        (m-2) + (col(i)-1)*m...
        - col(i) + 2],row(i)*2) == 1);
    A((c-1) + (col(i)-1)*m - col(i) + 2,:) = 0;
    B((c-1) + (col(i)-1)*m - col(i) + 2,:) = 0;
end

%%
% Define the function that we want to optimize.

Q = sym('a',[1,2*m]);
f3 = 0;
for i = 1:m
    f1 = g(i)*Q(2*i-1);
    f2 = a(i).*Q(2*i-1)/Q(2*i);
    f3 = f3 + f1 + f2;
end

T = matlabFunction(f3,'vars',{Q});
%%
% The final step is to use fmincon to
% solve the constrained optimization problem.
% Solution is in order R1,r1,R2,r2,....

lb = zeros(1,2*m);
ub = [];
```

```
x0 = zeros(1,2*m);
x0 = x0 + 5;

x = fmincon(T,x0,A,B,[],[],lb,ub)

%%
%For 2D problems the below code will plot the solution.

if(n == 2)
    ang=0:0.01:2*pi;
    hold on
    for i = 1:m

        xp=x(2*i-1)*cos(ang);
        yp=x(2*i-1)*sin(ang);
        xxp=x(2*i)*cos(ang);
        yyp=x(2*i)*sin(ang);
        set(gca, 'ColorOrderIndex', i)
        plot(P(1,i)+xp,P(2,i)+yp);
        set(gca, 'ColorOrderIndex', i)
        plot(P(1,i)+xxp,P(2,i)+yyp);
        set(gca, 'ColorOrderIndex', i)
        plot(P(1,i),P(2,i),'*','MarkerSize',12);

    end
    axis equal
    set(gcf,'Position',[200 200 3.45*96 2.25*96])
```

```
    set(gca,'FontName','Times')
    set(gca,'FontSize',8)
    hold off
else
end
```

Level Set Sizes. This code obtains each Lyapunov level set size from the ball sizes and eigenvalues.

```
function [L,l,K] = reslevsets(x,lammin,lammax,m)
%%
% Obtain all level set sizes using minimum
% and maximum eigenvalues obtained in resweights.

L = zeros(1,m);
l = zeros(1,m);
K = zeros(1,m);
for i = 1:m
    L(i) = (lammax(i)).*((x(2.*i - 1)).^2);
    l(i) = (lammin(i)).*((x(2.*i)).^2);
end

for i = 1:m
   K(i) = (log(l(i)/L(i)))...
   /(log(((x(2.*i)).^2)/((x(2.*i - 1)).^2)));
end
```

Dwell Times. Finally, the dwell times are calculated from all previous information.

```
function [waits] = restimes(L,l,timeconstants,m)
waits = zeros(1,m).';
for i = 1:m
    waits(i) = (log((l(i))/(L(i))))*(-timeconstants(i));
end
end
```

Settling Time Main. This serves as an alternative main function file that uses the settling time approach to produce dwell times.

```
%Main
clc
clearvars
%%
% The only inputs are all the system
% dynamics from fxu.m, and
% the input matrix,
% U, which defines the system modes.
% The U matrix should have
% an input going down a column,
% with the number
% of columns corresponding to the
% discrete number of inputs
% (and thus modes).
dim = 2;
U = [30,500]; %Boost Converter Inputs

% Obtain operating points and linearizations.
```

```
% Columns of 'modes' are operating points,
% number of rows is the dimension. A is an array where A{i}
% is the linearization matrix of the ith mode.

[A,gam,modes,maxeigs] = resgamv2(U,dim);

%%
% Obtain number of subsystems.
m = length(modes(1,:));

%%
% This section sets up the path matrix,
% Mark. That is, this
% matrix shows whether or not a path exists
% from mode x to
% mode y. If there is no path from x to y,
% then the big ball
% of x mustn't contain the small of y,
% and so we can use that
% info to tailor our constraints to the problem.
% Mark(1,3) = 0 implies that there is no path from mode 1.
% to mode 3.

Mark = ones([m,m]);

%%
% Determine the optimal size of all of the
```

```
% radii for the balls to be used for dwell times.
alpha = 1./maxeigs;
[radii] = resballs(modes, alpha, gam, Mark);

%%
% Obtain dwell times from settling times
[dwelltimes, perc] = ressettle(radii, maxeigs, m)
```

Settling Times. This code computes dwell times using the settling time method.

```
function [dwelltimes, perc] = ressettle(radii, maxeigs, m)

dwelltimes = zeros(1,m);
perc = zeros(1,m);
for i = 1:m
    perc(i) = radii(2*i)/radii(2*i - 1);
    dwelltimes(i) = abs(log(perc(i)))/maxeigs(i);
end
```

REFERENCES

[1] D. Liberzon, *Switching in Systems and Control*. New York, NY: Birkhäuser, 2003.

[2] J. P. Hespanha and A. S. Morse, "Stability of switched systems with average dwell time," in *38th Conference on Decision and Control*, 1999.

[3] D. Liberzon and A. S. Morse, "Basic problems in stability and design of switched systems," *IEEE Control Systems Magazine*, vol. 19, October 1999.

[4] X. Gao, D. Liberzon, J. Liu, and T. Basar, "Unified stability criteria for slowly time-varying and switched linear systems," *Automatica*, 2018.

[5] X. Zhao, L. Zhang, P. Shi, and M. Liu, "Stability and stabilization of switched linear systems with mode-dependent average dwell time," *IEEE Transactions on Automatic Control*, vol. 57, pp. 1809–1815, July 2012.

[6] X. Zhao, S. Yin, H. Li, and B. Niu, "Switching stabilization for a class of slowly switched systems," *IEEE Transactions on Automatic Control*, vol. 60, pp. 221–226, 2015.

[7] M. S. Branicky, "Multiple lyapunov functions and other analysis tools for switched and hybrid systems," *IEEE Transactions on Automatic Control*, vol. 43, pp. 475–482, April 1998.

[8] J. C. Geromel and P. Colaneri, "Stability and stabilization of continuous-time switched linear systems," *IEEE Control Systems Magazine*, vol. 45, no. 5, pp. 1915–1930, 2006.

[9] A. Kundu and D. Chatterjee, "Stabilizing switching signals for switched systems," *IEEE Transactions on Automatic Control*, vol. 60, pp. 882–888, March 2015.

[10] J. Lee and G. E. Dullerud, "Uniformly stabilizing sets of switching sequences for switched linear systems," *IEEE Transactions on Automatic Control*, vol. 52, pp. 868–874, May 2007.

[11] R. A. Decarlo, M. S. Branicky, S. Pettersson, and B. Lennartson, "Perspectives and results on the stability and stabilizability of hybrid systems," *Proceedings of the IEEE*, vol. 88, no. 7, pp. 1069–1082, July 2000.

[12] G. Davrazos and N. T. Koussoulas, "A review of stability results for switched and hybrid systems," in *Proc. 9th Mediterranean Conference on Control and Automation*, 2001.

[13] H. Lin and P. J. Antsaklis, "Stability and stabilizability of switched linear systems: A survey of recent results," *IEEE Transactions on Automatic Control*, vol. 54, pp. 308–322, February 2009.

[14] X. Xu and G. Zhai, "Practical stability and stabilization of hybrid and switched systems," *IEEE Transactions on Automatic Control*, vol. 50, no. 11, pp. 1897–1903, Nov 2005.

[15] G. Zhai and A. N. Michel, "Generalized practical stability analysis of discontinuous dynamical systems," in *42nd IEEE International Conference on Decision and Control (IEEE Cat. No.03CH37475)*, vol. 2, Dec 2003, pp. 1663–1668 Vol.2.

[16] T. Alpcan and T. Basar, "A stability result for switched systems with multiple equilibria," *Dynamics of Continuous, Discrete, and Impulsive Systems*, vol. 17, pp. 949–958, May 2010.

[17] F. Blanchini, D. Casagrande, and S. Miani, "Modal and transition dwell time computation in switching systems: A set-theoretic approach," *Automatica*, vol. 46, pp. 1477–1482, July 2010.

[18] R. Kuiava, R. A. Ramos, H. R. Pota, and L. F. C. Alberto, "Practical stability of continuous-time switched systems without a common equilibria and governed by a time-dependent switching signal," in *2011 9th IEEE International Conference on Control and Automation (ICCA)*, Dec 2011, pp. 1156–1161.

[19] R. Kuiava, R. A. Ramos, L. F. C. Alberto, and H. R. Pota, "Practical stability assessement of distributed synchronous generators under load variations," in *2013 IEEE International Symposium on Circuits and Systems (ISCAS2013)*, May 2013, pp. 457–460.

[20] G. Chesi, P. Colaneri, J. C. Geromel, and R. Middleton, "Computing upper-bounds of the minimum dwell time of linear switched systems via homogeneous polynomial lyapunov functions," in *American Control Conference Proc.*, 2010, pp. 2487–2492.

[21] H. K. Khalil, *Nonlinear Systems*. Upper Saddle River, NJ: Prentice Hall, 2001.

[22] M. Caramia and P. Dell'Olmo, *Multi-objective Management in Freight Logistics*. London, UK: Springer-Verlag, 2008.

[23] R. Krishnan, *Electric Motor Drives: Modeling, Analysis, and Control*. Upper Saddle River, NJ: Prentice Hall, 2001.

[24] P. C. Krause, O. Wasynczuk, and S. D. Sudhoff, *Analysis of Electric Machinery and Drive Systems*, 2nd ed. Piscataway, NJ: IEEE Press, 2002.

[25] M. Rasheduzzaman, J. A. Mueller, and J. W. Kimball, "An accurate small-signal model of inverter-dominated islanded microgrids using dq reference frame," *IEEE Journal of Emerging and Selected Topics in Power Electronics*, vol. 2, December 2014.

[26] Z. Gajić and M. T. J. Qureshi, *Lyapunov Matrix Equation in System Stability and Control*. San Diego, CA: Academic Press, 1995.

[27] H. G. Kwatny and G. L. Blankenship, *Nonlinear Control and Analytical Mechanics*. New York, NY: Birkhäuser, 2000.

VITA

William St. Pierre received his Bachelor of Arts in mathematics from Truman State University in Kirksville, Missouri in May 2016. He proceeded to pursue a Master of Science in electrical engineering from Missouri University of Science and Technology in Rolla, Missouri. His research interests included switched system stability, optimal control of switched systems, and microgrid modelling and control.

In December 2018, he received his Master of Science in electrical engineering from Missouri University of Science and Technology.